Electronic Supplementary Material (ESI) for Dalton Transactions.
This journal is © The Royal Society of Chemistry 2021

# The Influence of Ring Strain on the Formation of Si-H-Si Stabilised Oligosilanylsilyl Cations

# - Supporting Information –

Jelte P. Nimoth and Thomas Müller*

## General Aspects

### Preparation of Glass Ware and Solvents

For all cation preparations, common Schlenk techniques were applied. As protective gas, nitrogen 5.0 was used. All glassware was heated in an oven at 160 °C, evacuated while hot and then flushed with nitrogen. For anhydrous non-deuterated solvents, the following drying procedures were applied: THF was first stirred over NaOH, distilled, and then dried by refluxing over Na/K alloy followed by distillation. Diethyl ether was also dried by refluxing over Na/K alloy followed by distillation. Dichloromethane was refluxed over $CaH_2$ and then distilled.

### NMR Spectroscopy

Deuterated NMR solvents and the non-deuterated 3-F-toluene (3-F-tol) were dried over 4 Å molecular sieve. In those cases where 3-F-tol was used as solvent, a capillary with acetone-$d_6$ inside the tube was used as lock solvent. $^1H$ NMR spectra were referenced to the residual protons of the deuterated solvent as internal reference (Table S 1). $^{13}C$ NMR spectra were referenced to the central line of the solvent signal when deuterated solvents were applied (Table S 1). In case of 3-F-tol, the signals were calibrated against the $^1H$ and $^{13}C$ NMR shifts of its methyl group relative to tetramethylsilane (TMS) used as an internal standard in neat 3-F-tol.

**Table S 1. NMR chemical shifts of solvents used as reference.**[1]

| Solvent | $\delta^1H$[a] | $\delta^{13}C$ |
|---|---|---|
| Chloroform-d | 7.26 | 77.2 |
| Dichloromethane-$d_2$ | 5.32 | 53.9 |
| 3-Fluorotoluene[b] | 2.13 | 21.0 |

[a] NMR shift of the residual protons of the deuterated solvents (except 3-F-tol). [b] NMR shifts referenced versus $CH_3$ group of neat 3-F-tol using TMS as internal standard (TMS: $\delta^1H = 0.00$, $\delta^{13}C = 0.0$).

Other heteronuclear NMR spectra ($^{11}B$, $^{19}F$, $^{29}Si$) were calibrated against external standards (Table S 2).

**Table S 2. External standard used for calibration of heteronuclear NMR spectra.**

| NMR Nucleus | External Standard | Reference |
|---|---|---|
| $^{11}B$ | $BF_3 \cdot OEt_2$ | 0.0 |
| $^{19}F$ | $CFCl_3$ | 0.0 |
| $^{29}Si$ | $Me_2HSiCl$ | 11.1[a] |

[a] Referenced vs. TMS ($\delta^{29}Si = 0.0$)

All NMR spectra were executed and analysed using the Mestrelab MestReNova NMR software (Version 9.1.0-14011). The FIDs (free induction decay) of the heteronuclear 1D NMR spectra were folded with an exponential function using the window function routine of the NMR software and the exponential factors (em) of em = 2.00-10.00. For 1D $^{1}$H NMR spectra, em = 0.30 was used. If other em or gauss multiplications (gm) were used, it is specified beneath the respective spectra. The $^{29}$Si and $^{29}$Si{$^{1}$H} NMR spectra were recorded with a relaxation delay of D1 = 10 s, while D1 = 3 s was used for $^{29}$Si{$^{1}$H} INEPT NMR spectra. The $^{29}$Si{$^{1}$H} INEPT NMR spectra were obtained using values of $J$ = 8 Hz, n = 6 for $SiMe_2$ groups or $J$ = 9 Hz, n = 9 for $SiMe_3$ groups. The $^{1}$H,$^{29}$Si HMQC spectra and $^{1}$H,$^{29}$Si HMBC spectra were obtained for $J$ = 180 Hz and $J$ = 8 Hz, respectively. $^{1}$H,$^{13}$C HMQC spectra and $^{1}$H, $^{13}$C HMBC spectra were obtained using settings for $J$ = 145 Hz and $J$ = 8 Hz, respectively. The 2D NMR spectra were processed using window functions of sine square 0.00° in both dimensions for $^{1}$H,$^{13}$C HMQC and $^{1}$H,$^{29}$Si HMQC/HMBC. For $^{1}$H,$^{1}$H COSY NMR spectra and $^{1}$H,$^{13}$C HMBC NMR spectra windows function of sine bell 0.00° in both dimensions were used. Deviating processing settings are marked beneath the respective 2D NMR spectra.

**Gas Chromatography-Mass Spectrometry (GCMS)**

GCMS data were obtained on an Agilent 7890B with Agilent 5977B GC/MSD detection unit (stationary phase: HP-5MS UI column, length 30 m, diameter 0.25 mm, film thickness 0.25 µm).

# Synthesis of starting materials

## Synthesis and NMR Data of $Si(SiMe_3)_4$ (6)

$$SiCl_4 \quad + \quad 4\ Me_3SiCl \xrightarrow[\text{THF, 0 °C to r.t, 16 h} \atop \text{- 8 LiCl}]{\text{Li}} Si(SiMe_3)_4$$

**6**

In a three-neck glass flask equipped with a dropping funnel, Li (12.00 equiv., 1.25 mol, 8.66 g) was suspended in THF (135 mL) and the suspension was cooled to 0 °C by cooling bath. $Me_3SiCl$ (4.80 equiv., 499.1 mmol, 54.23 g) was added via syringe. Subsequently, $SiCl_4$ (1.00 equiv., 103.9 mmol, 17.67 g) was dissolved in THF (120 mL) and added dropwise over the course of 1.5 h. The resulting suspension was stirred for 16 h while gradually warming-up to room temperature. Excess Li and formed salts were filtered and the obtained solution was hydrolysed with 10% hydrochloric acid and ice. The aqueous phase was separated and neutralised by stepwise addition of $NaHCO_3$. It was then extracted with *n*-pentane (2 x 100 mL). The combined organic phases were dried over $Na_2SO_4$ and the residue was recrystallised from ethanol. The oligosilane **6** was obtained as a colourless solid in 76 % yield (83.38 mmol, 26.11 g).

NMR spectroscopic data are in accordance with literature.[2]

$^{1}$H NMR ($CDCl_3$, 499.87 MHz, 305.0 K): 0.21 (s, $Si\underline{Me}_3$). $^{29}$Si{$^{1}$H} NMR ($CDCl_3$, 99.31 MHz, 305.0 K): –135.2 (s, $\underline{Si}Si_4$), –9.9 (s, $Si\underline{Me}_3$).

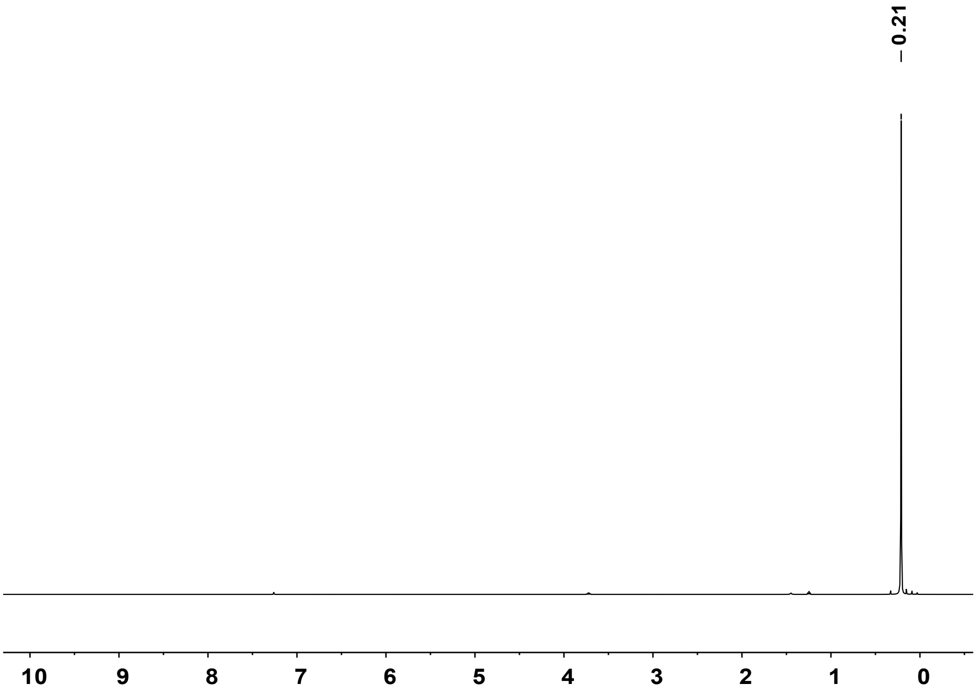

**Figure S 1.** $^1$H NMR spectrum of **6** ($CDCl_3$, 499.87 MHz, 305.0 K).

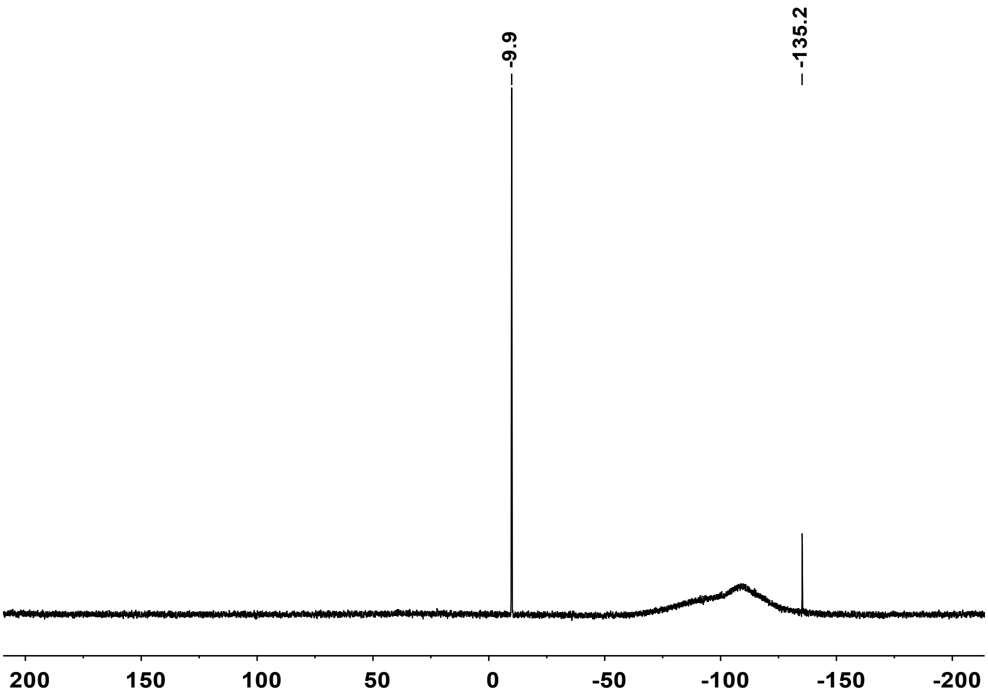

**Figure S 2.** $^{29}Si\{^1H\}$ NMR spectrum of **6** ($CDCl_3$, 99.31 MHz, 305.0 K).

## Synthesis and NMR Data of $Si(SiMe_2Cl)_4$ (7)

$$\underset{\mathbf{6}}{Si(SiMe_3)_4} \xrightarrow[CD_2Cl_2,\ r.t.,\ 16\ h]{AlCl_3/acetyl\ chloride} \underset{\mathbf{7}}{Si(SiMe_2Cl)_4}$$

The oligosilane **6** (1.00 equiv., 28.05 mmol, 9.00 g) and $AlCl_3$ (5.00 equiv., 112.21 mmol, 14.96 g) were dissolved in dichloromethane (100 mL). Acetyl chloride (5.00 equiv., 112.21 mmol, 8.81 g) was added and the reaction mixture was stirred for 16 h. Subsequently, the volatile components were removed under reduced pressure and the residue was extracted with n-pentane (3x 80 mL). After filtration, the solvent was removed under reduced pressure and **7** was obtained as a colourless solid in 81 % yield (22.86 mmol, 9.20 g).

NMR spectroscopic data are in accordance with literature.[3]

$^1$H NMR ($CDCl_3$, 499.87 MHz, 305.0 K): 0.75 (s, Si<u>Me</u>$_2$Cl). $^{13}$C{$^1$H} NMR ($CDCl_3$, 125.71 MHz, 305.0 K): 6.7 (s, Si<u>Me</u>$_2$Cl). $^{29}$Si{$^1$H} NMR ($CDCl_3$, 99.31 MHz, 305.0 K): –113.4 (s, <u>Si</u>Si$_4$), 27.8 (s, Si<u>Me</u>$_2$Cl).

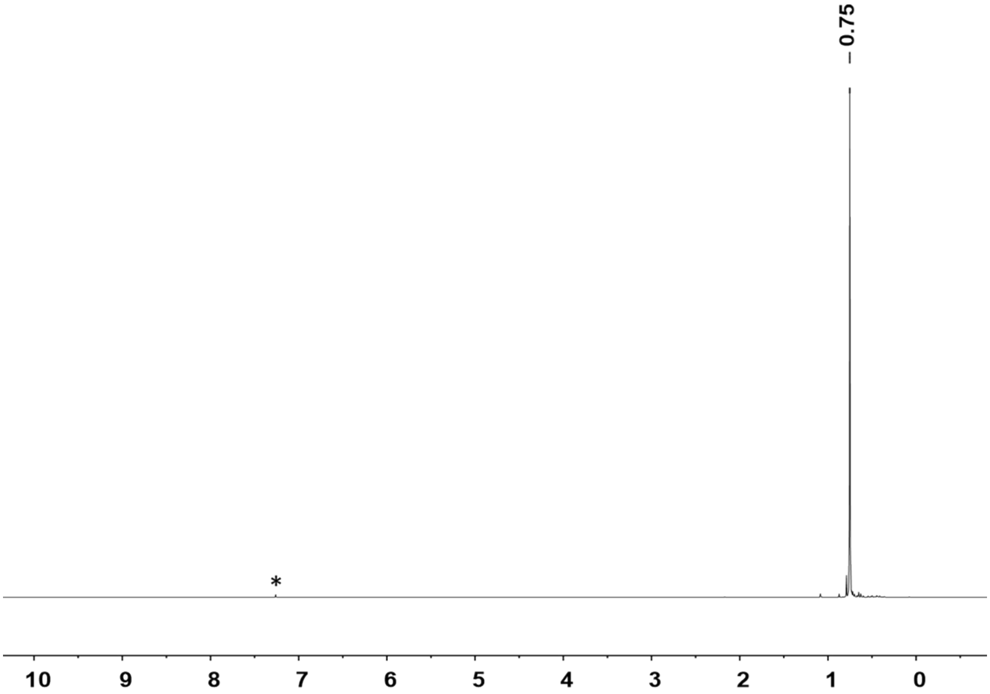

**Figure S 3.** $^1$H NMR spectrum of **7** ($CDCl_3$, 499.87 MHz, 305.0 K, * = $CHCl_3$).

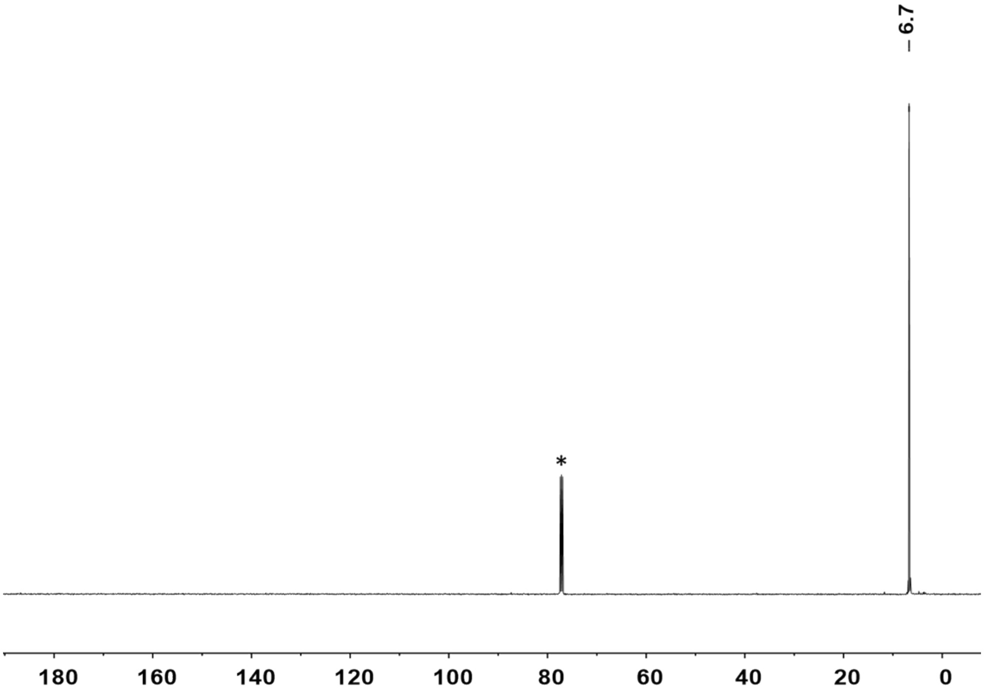

**Figure S 4.** $^{13}$C{$^1$H} NMR spectrum of **7** ($CDCl_3$, 125.71 MHz, 305.0 K, * = $CDCl_3$).

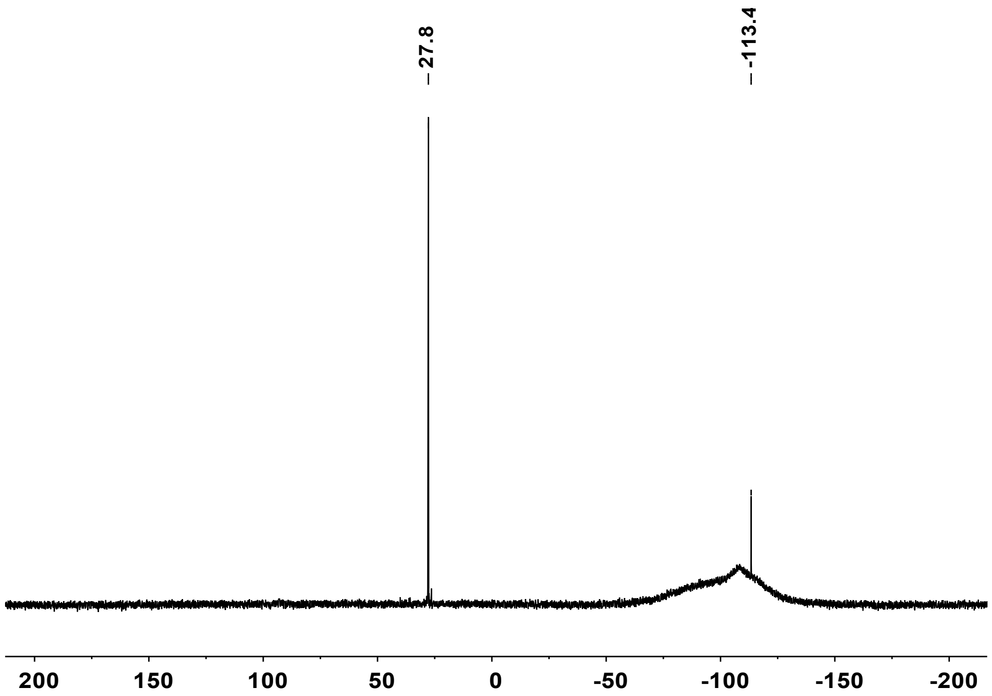

**Figure S 5.** $^{29}$Si{$^1$H} NMR spectrum of **7** ($CDCl_3$, 99.31 MHz, 305.0 K).

## Synthesis and NMR Data of $Si(SiMe_2H)_4$ (2)

$$\underset{\textbf{7}}{Si(SiMe_2Cl)_4} \xrightarrow[Et_2O,\ 0\ °C\ \text{to r.t, 16 h}]{Li[AlH_4]} \underset{\textbf{2}}{Si(SiMe_2H)_4}$$

The chlorinated oligosilane **7** (1.00 equiv., 4.08 mmol, 1.64 g) was dissolved in $Et_2O$ (30 mL). Subsequently, $Li[AlH_4]$ (4.00 equiv., 16.30 mmol) was added and the suspension was stirred for 16 h. The solvent was removed under reduced pressure. The residue was redissolved in n-pentane (40 mL) and filtered over a $D_4$ frit. After renewed removal of the solvent under reduced pressure, the oligosilane **2** was obtained as a colourless solid in 79 % yield (3.21 mmol, 0.85 g).

NMR spectroscopic data are in accordance with literature.[4, 5]

$^1$H NMR ($CD_2Cl_2$, 499.87 MHz, 197.9 K): 0.18 (d, $^3J_{H,H}$ = 4.4 Hz, Si$\underline{Me}_3$H), 3.91 (sept, $^3J_{H,H}$ = 4.4 Hz, $SiMe_3\underline{H}$). $^{29}$Si{$^1$H} NMR ($CD_2Cl_2$, 99.31 MHz, 198.0 K): –142.8 (s, $\underline{Si}Si_4$), –33.4 (s, Si$\underline{Me}_3$).

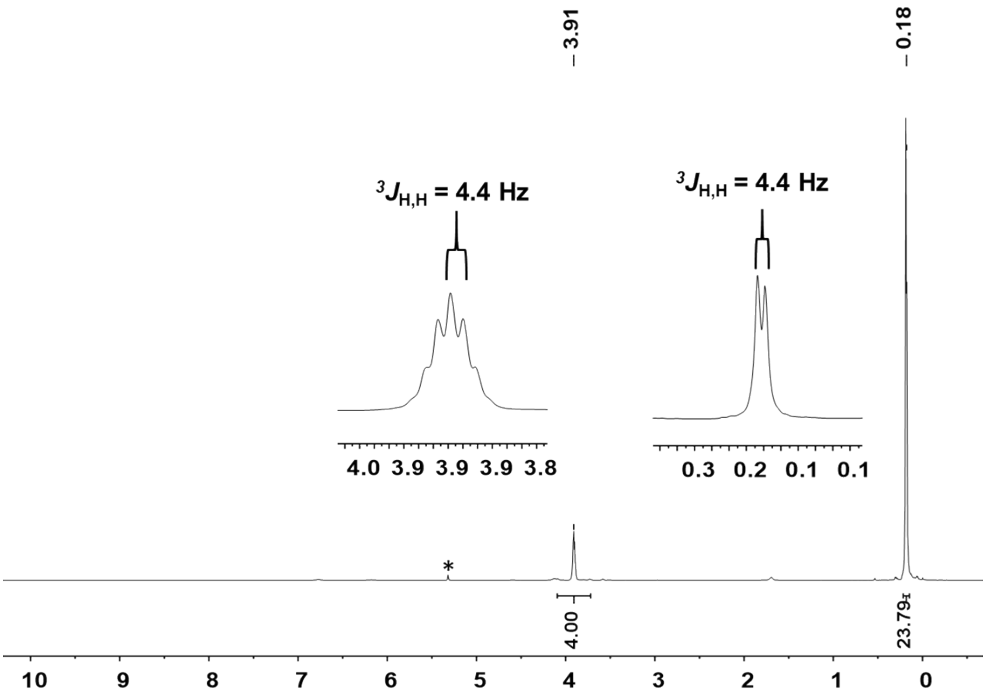

**Figure S 6.** $^1$H NMR spectrum of **2** ($CD_2Cl_2$, 499.87 MHz, 197.9 K, * = $CHDCl_2$).

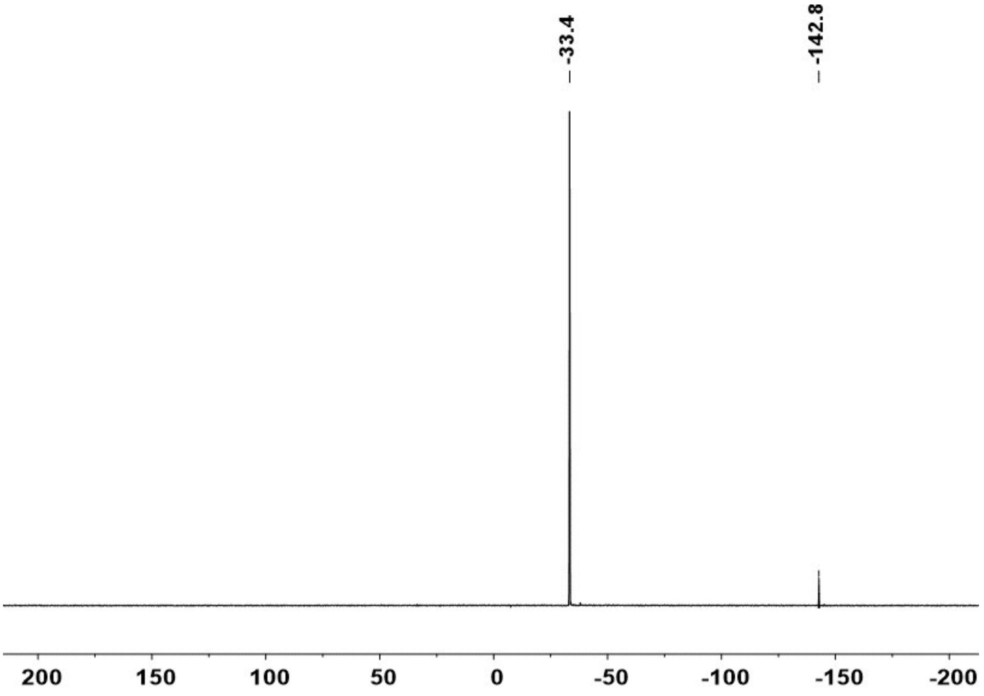

**Figure S 7.** $^{29}$Si{$^1$H} NMR spectrum of **2** ($CD_2Cl_2$, 99.31 MHz, 198.0 K).

# Cation Syntheses

## General Aspects

The starting material $Si(SiMe_2H)_4$ (**2**) was distilled prior of its use in the hydride transfer reactions with $[Ph_3C][B(C_6F_5)_4]$.

$[Ph_3C][B(C_6F_5)_4]$ was synthesised according to a slightly modified literature procedure.[6] In contrast to the original literature, the initially formed $Li[B(C_6F_5)_4]$ was washed with *n*-pentane, redissolved in dichloromethane and $Ph_3CCl$ was added to the dichloromethane solution to form $[Ph_3C][B(C_6F_5)_4]$.

A general procedure was used for the hydride transfer reaction between **2** and $[Ph_3C][B(C_6F_5)_4]$. The reaction was performed directly in the NMR tube using specifically designed glass ware. The tube was charged with the respective amount of $[Ph_3C][B(C_6F_5)_4]$ and evacuated for 30 min. Afterwards, 0.3 mL of the used NMR solvent were added, and the solution was cooled to the reaction temperature. Subsequently, a solution of **2** in the NMR solvent was slowly added via syringe. By careful addition, a two phasic mixture was obtained. The NMR tube was sealed, the sample was mixed and then transferred to the precooled NMR spectrometer.

If non-deuterated 3-fluorotoluene was used as solvent, a sealed glass capillary filled with acetone-$d_6$ was added to the NMR tube to establish NMR lock.

### Reaction conditions: DCM, –90 °C, 0.5 equiv. $[Ph_3C][B(C_6F_5)_4]$

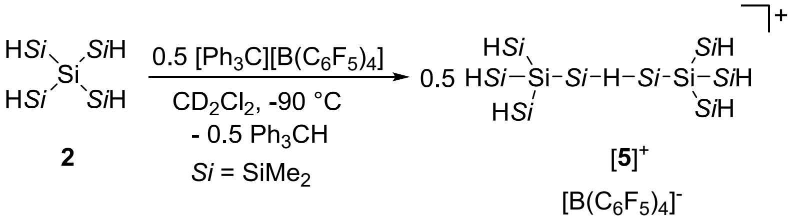

The general procedure was applied for the hydride transfer reaction between pentasilane **2** and $[Ph_3C][B(C_6F_5)_4]$ in dichloromethane-$d_2$. The trityl salt, $[Ph_3C][B(C_6F_5)_4]$ (1.00 equiv., 0.07 mmol), was dissolved in dichloromethane-$d_2$ (0.3 mL) in an NMR tube and cooled down. Subsequently, a solution of silane **2** (1.00 equiv., 0.07 mmol) in dichloromethane-$d_2$ (0.3 mL) was slowly added at –90 °C via syringe. The spectroscopic data showed the formation of one main product which was correlated to the intermolecularly stabilised silyl cation [**5**]$^+$ (compare reactions in 3-F-tol).

Analytical data of [**5**]$[B(C_6F_5)_4]$

$^{1}H$ NMR ($CD_2Cl_2$, 499.87 MHz, 183.0 K): No signals assigned. $^{13}C\{^{1}H\}$ NMR ($CD_2Cl_2$, 125.71 MHz, 183.0 K): No signals assigned. $^{29}Si\{^{1}H\}$ NMR ($CD_2Cl_2$, 99.31 MHz, 183.0 K): –133.0 (bs, $SiSi_4$), –32.6 (s, $SiMe_2H$), 93.9 (bs, $Me_2Si$-H-$SiMe_2$). $^{29}Si$ NMR ($CD_2Cl_2$, 99.31 MHz, 182.9 K): –133.0 (bs, $SiSi_4$), –32.6 (d, $^{1}J_{Si,H}$ = 185 MHz, $SiMe_2H$), 93.9 (bm, $Me_2Si$-H-$SiMe_2$).

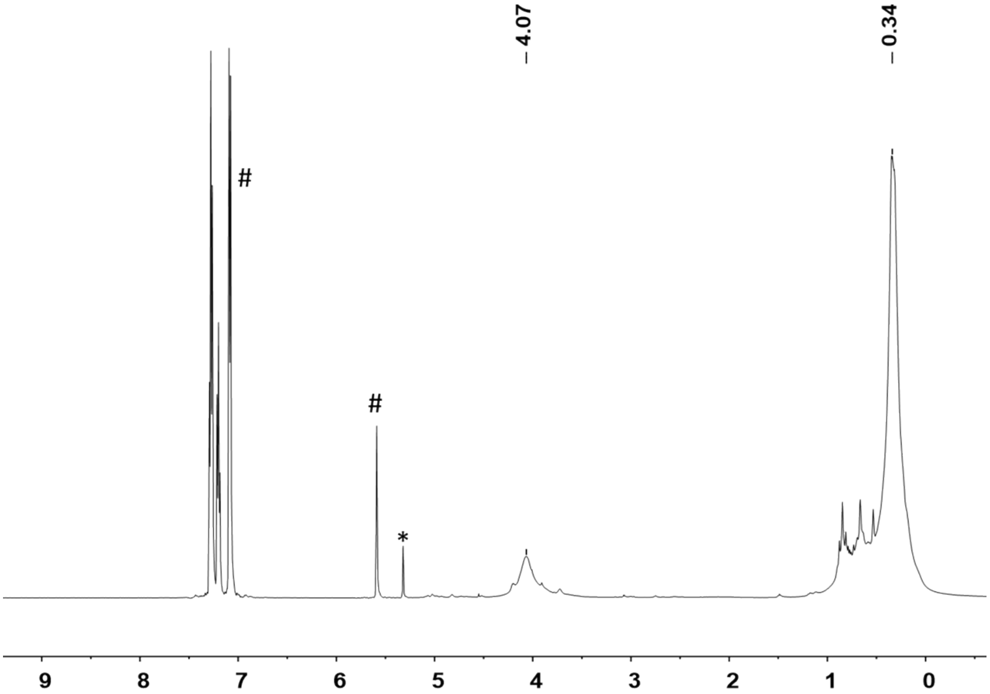

**Figure S 8.** $^1$H NMR spectrum of [**5**][B($C_6F_5$)$_4$] ($CD_2Cl_2$, 499.87 MHz, 183.0 K, * = $CHDCl_2$, # = $Ph_3CH$).

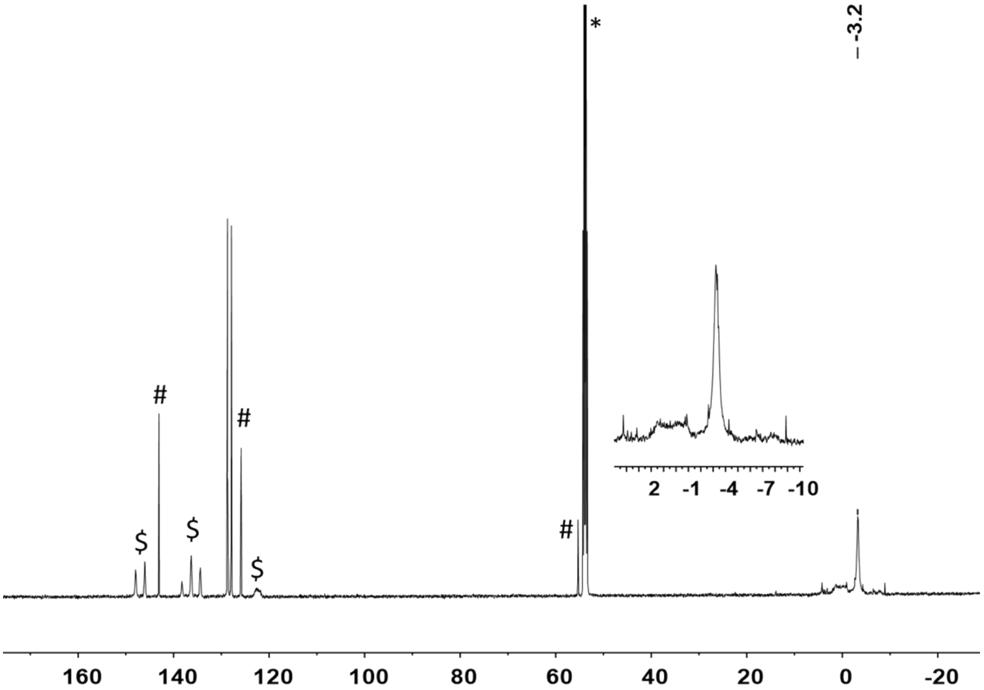

**Figure S 9.** $^{13}$C{$^1$H} NMR spectrum of [**5**][B($C_6F_5$)$_4$] ($CD_2Cl_2$, 125.71 MHz, 183.0 K, * = $CD_2Cl_2$, # = $Ph_3CH$, $ = [B($C_6F_5$)$_4$]$^-$).

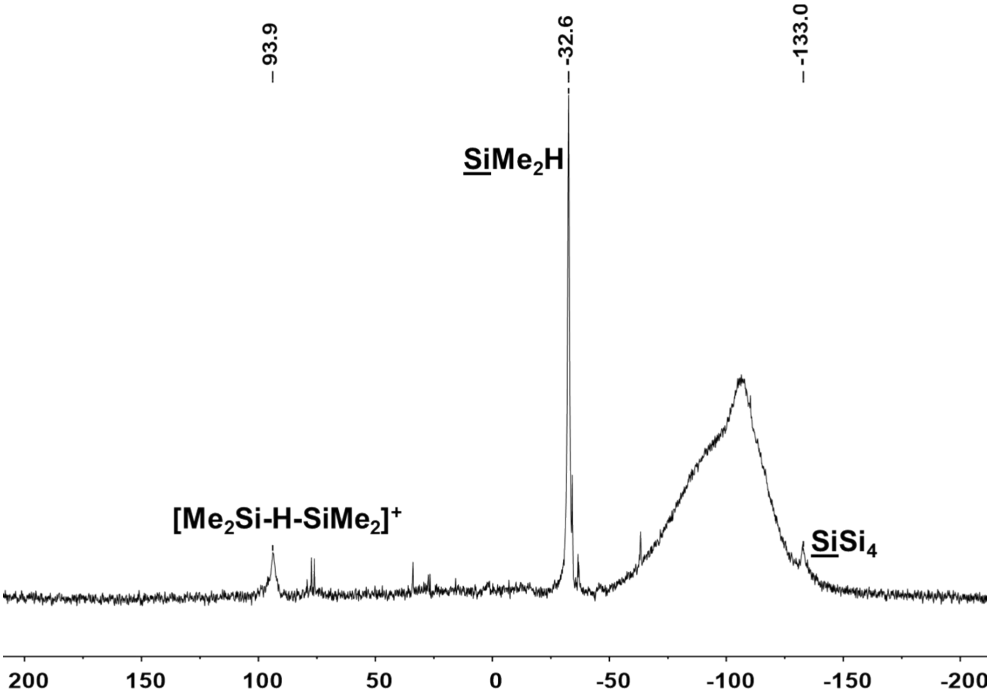

**Figure S 10.** $^{29}$Si{$^1$H} NMR spectrum of [**5**][B(C$_6$F$_5$)$_4$] (CD$_2$Cl$_2$, 99.31 MHz, 183.0 K).

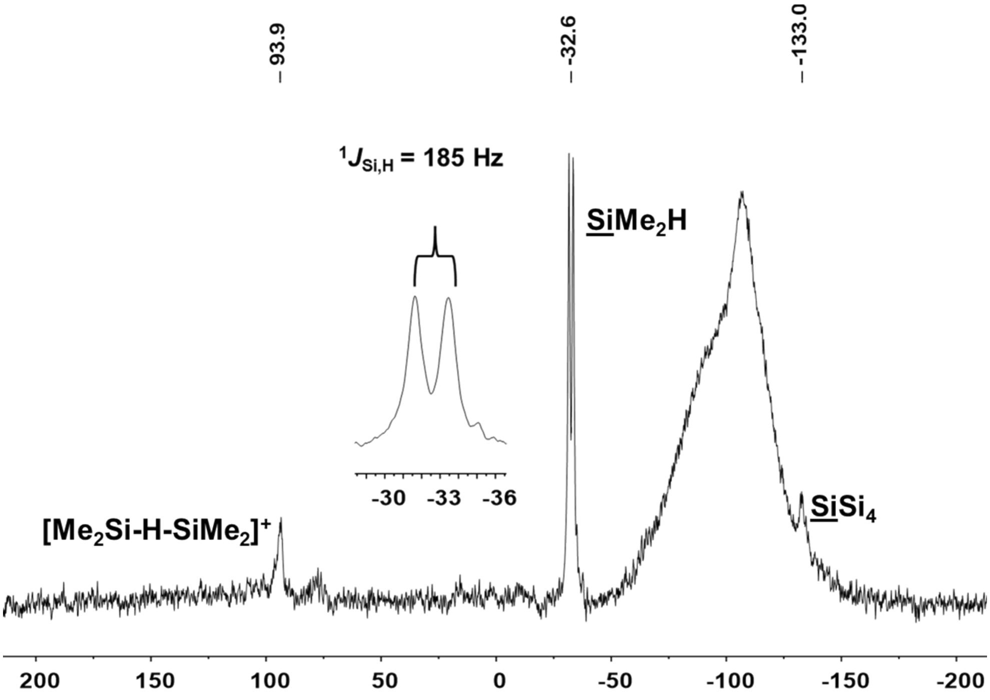

**Figure S 11.** $^{29}$Si NMR spectrum of [**5**][B(C$_6$F$_5$)$_4$] (CD$_2$Cl$_2$, 99.31 MHz, 182.9 K).

**Reaction conditions: DCM, –90 °C, 1.0 equiv. $[Ph_3C][B(C_6F_5)_4]$**

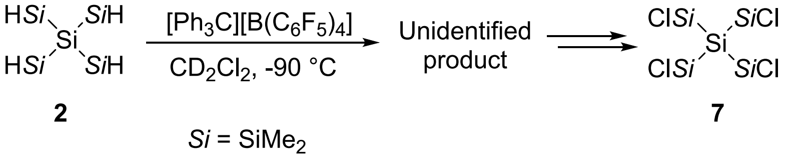

The general procedure was applied for the hydride transfer reaction between pentasilane **2** and $[Ph_3C][B(C_6F_5)_4]$ in dichloromethane. The trityl salt, $[Ph_3C][B(C_6F_5)_4]$ (1.00 equiv., 0.13 mmol), was dissolved in dichloromethane-$d_2$ (0.3 mL) in an NMR tube and cooled down. Subsequently, a solution of silane **2** (1.00 equiv., 0.13 mmol) in dichloromethane-$d_2$ (0.3 mL) was slowly added at –90 °C via syringe. Instead of the formation of [**5**]$[B(C_6F_5)_4]$, the NMR spectra showed a multitude of signals from which no structure could be elucidated. Renewed mixing of the NMR sample accompanied by a slight warming of the sample resulted in the formation of $Si(SiMe_2Cl)_4$ (**7**). Next to left-over trityl cation, the decomposition of the $Ph_3CH$, which was formed during hydride transfer reaction, was visible in the NMR data. The analytical data (NMR spectra and GCMS) agreed with the formation of the chlorosilane **7**.[3]

Analytical data of **7**

$^1$H NMR ($CD_2Cl_2$, 499.87 MHz, 183.0 K): 0.69 (s, Si$\underline{Me_2}$Cl). $^{13}$C{$^1$H} NMR ($CD_2Cl_2$, 125.71 MHz, 183.6 K): 5.3 (s, Si$\underline{Me_2}$Cl). $^{29}$Si{$^1$H} NMR ($CD_2Cl_2$, 99.31 MHz, 183.0 K): 28.7 (s, $\underline{Si}$Me$_2$Cl), –117.2 (s, $\underline{Si}$Si$_4$). $^{29}$Si INEPT NMR ($CD_2Cl_2$, 99.31 MHz, 183.0 K): 28.7 (m, $\underline{Si}$Me$_2$Cl), –117.2 (bs, $\underline{Si}$Si$_4$).

Mass required for $C_8H_{24}Cl_4Si_5$ (**7**): 399.95. Mass found: 387.00 (7) [$M^+$ -$CH_3$], 367.00 (10) [$M^+$ -$C_2H_6$], 309.00 (35) [$M^+$ -$C_2H_6ClSi$], 272.1 (100) [$M^+$ -$C_2H_6Cl_2Si$], 174.1 (56) [$M^+$ -$C_2H_6Cl_3Si$], 93.00 (39) [$C_2H_6ClSi^+$].

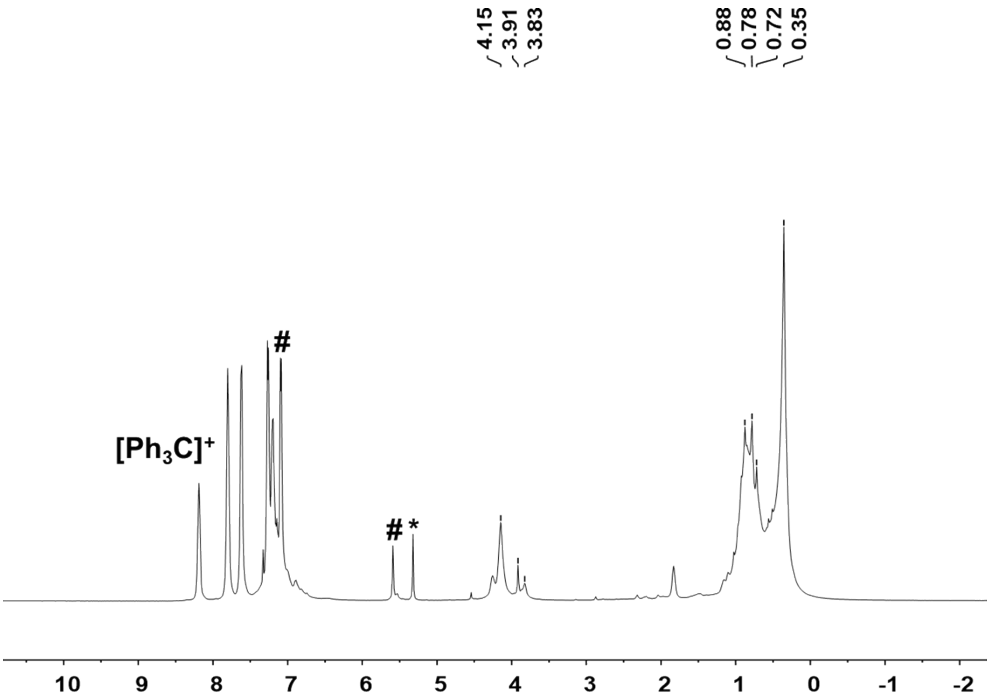

**Figure S 12.** $^1$H NMR spectrum prior to renewed mixing ($CD_2Cl_2$, 499.87 MHz, 183.0 K, * = $CHDCl_2$, # = $Ph_3CH$).

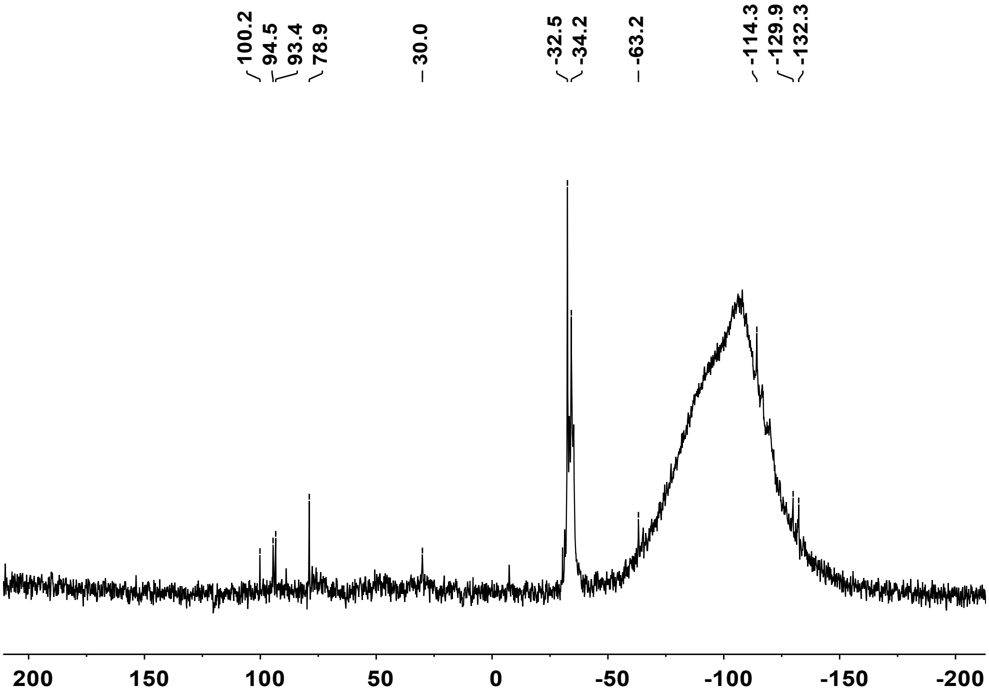

**Figure S 13.** $^{29}Si\{^{1}H\}$ NMR spectrum prior to renewed mixing ($CD_2Cl_2$, 99.31 MHz, 183.0 K).

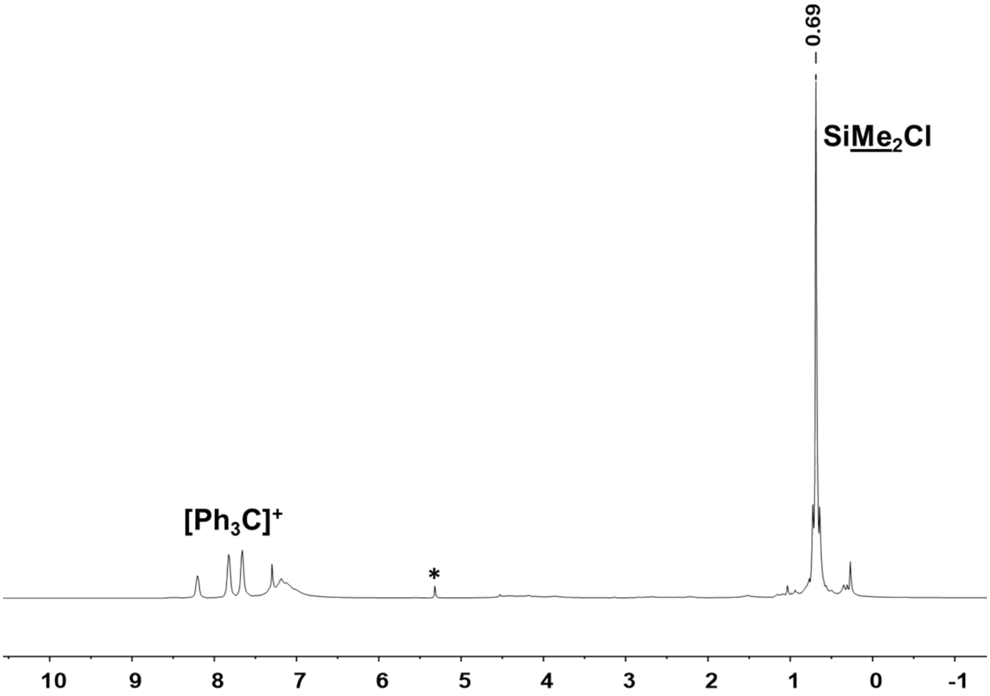

**Figure S 14.** $^{1}H$ NMR spectrum after renewed mixing ($CD_2Cl_2$, 499.87 MHz, 183.0 K, * = $CHDCl_2$).

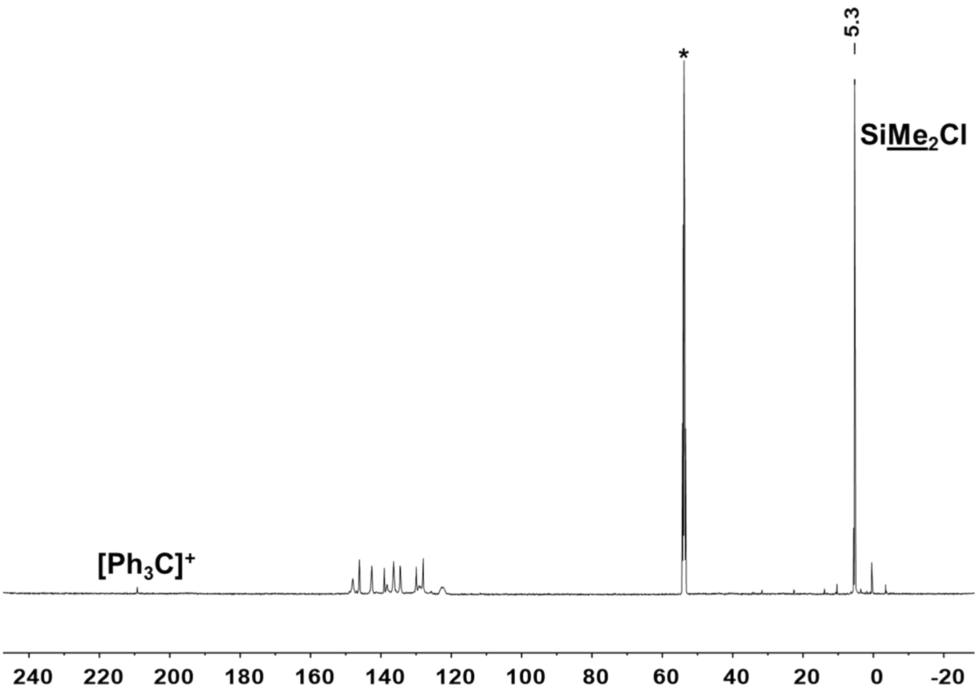

**Figure S 15.** $^{13}C\{^1H\}$ NMR spectrum after renewed mixing ($CD_2Cl_2$, 125.71 MHz, 183.6 K, * = $CD_2Cl_2$).

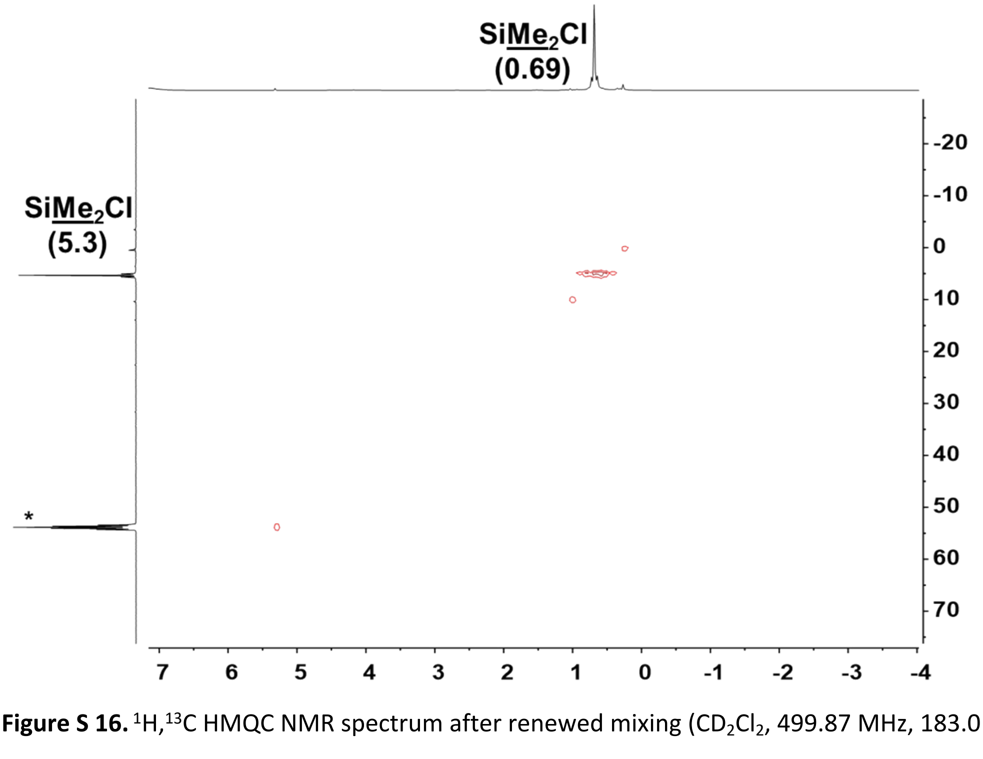

**Figure S 16.** $^1H,^{13}C$ HMQC NMR spectrum after renewed mixing ($CD_2Cl_2$, 499.87 MHz, 183.0 K, * = $CD_2Cl_2$).

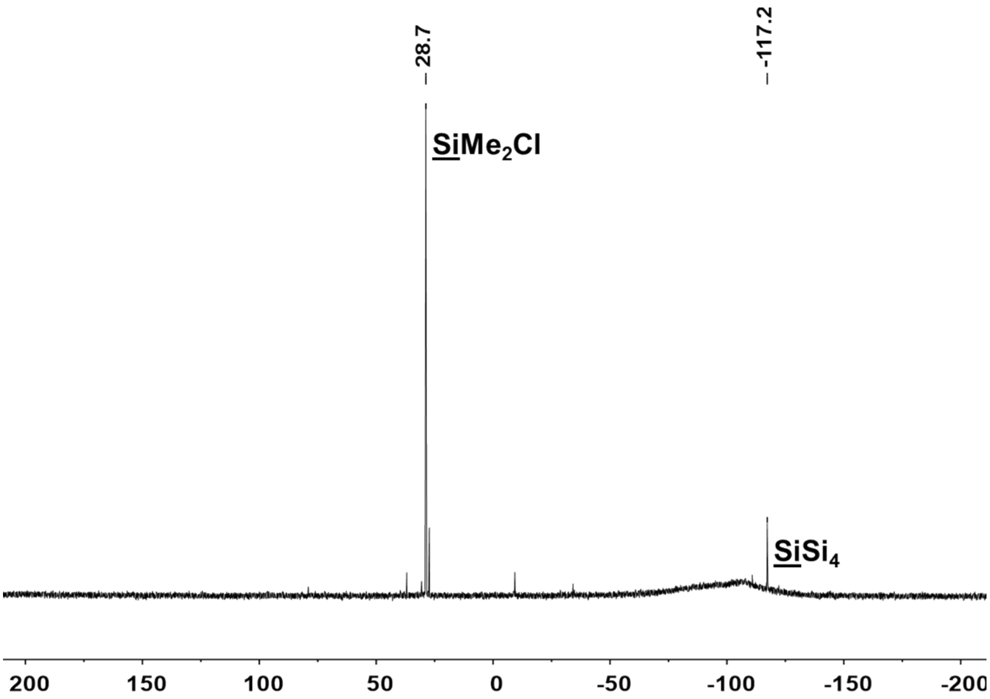

**Figure S 17.** $^{29}Si\{^1H\}$ NMR spectrum after renewed mixing ($CD_2Cl_2$, 99.31 MHz, 183.0 K).

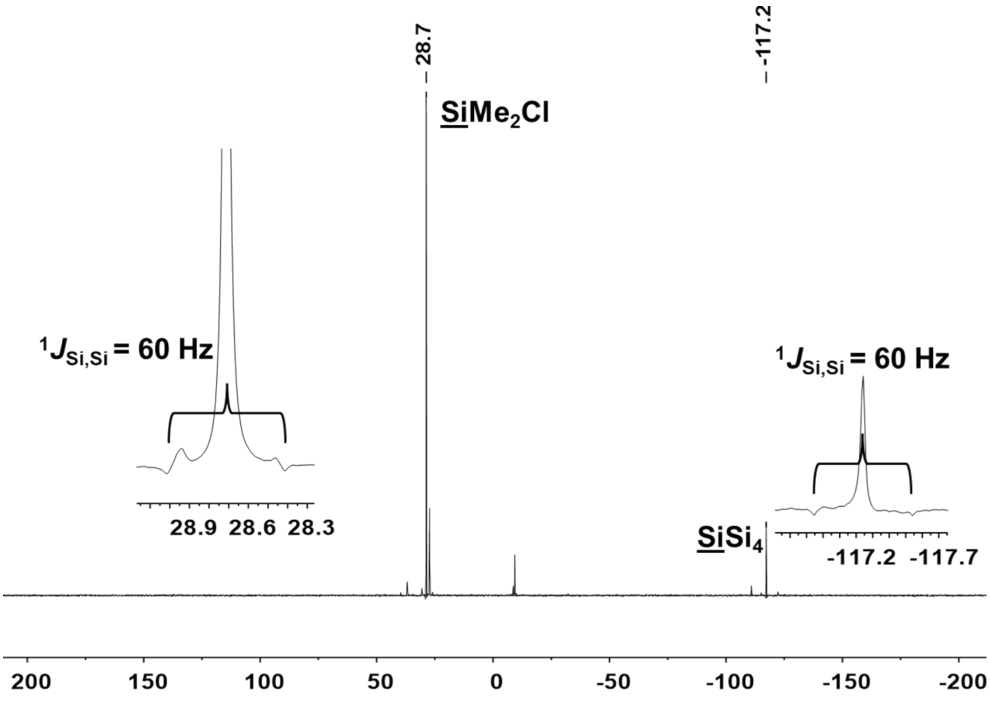

**Figure S 18.** $^{29}Si\{^1H\}$ INEPT NMR spectrum after renewed mixing ($CD_2Cl_2$, 99.31 MHz, 183.0 K).

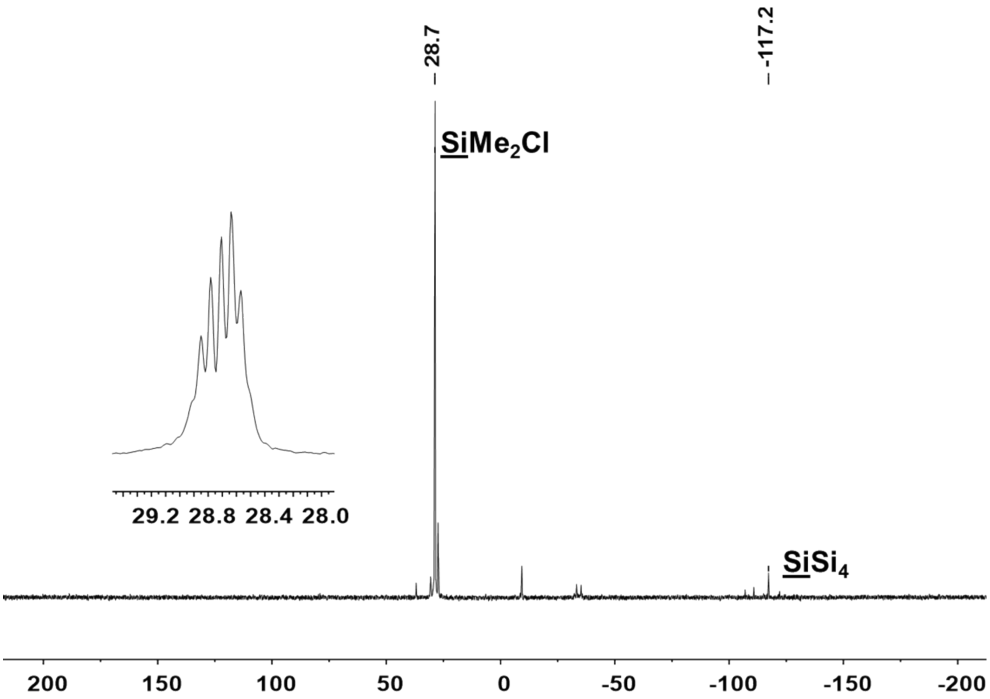

**Figure S 19.** $^{29}$Si INEPT NMR spectrum after renewed mixing ($CD_2Cl_2$, 99.31 MHz, 183.0 K, recorded with parameters for *J* = 40 Hz and n = 1).

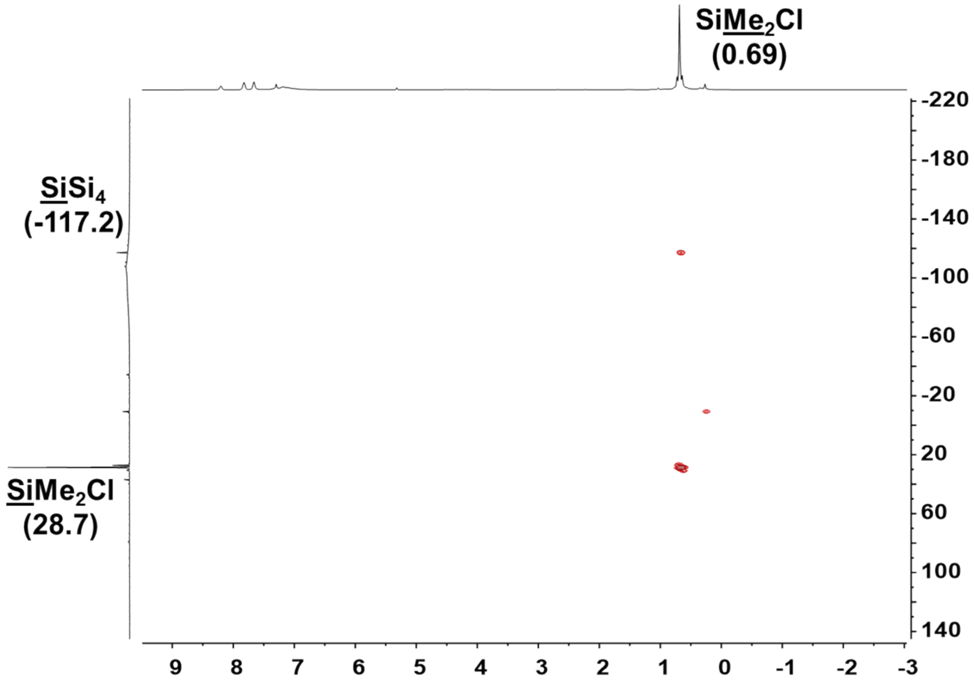

**Figure S 20.** $^1$H,$^{29}$Si HMBC NMR spectrum after renewed mixing ($CD_2Cl_2$, 499.87 MHz, 183.0 K).

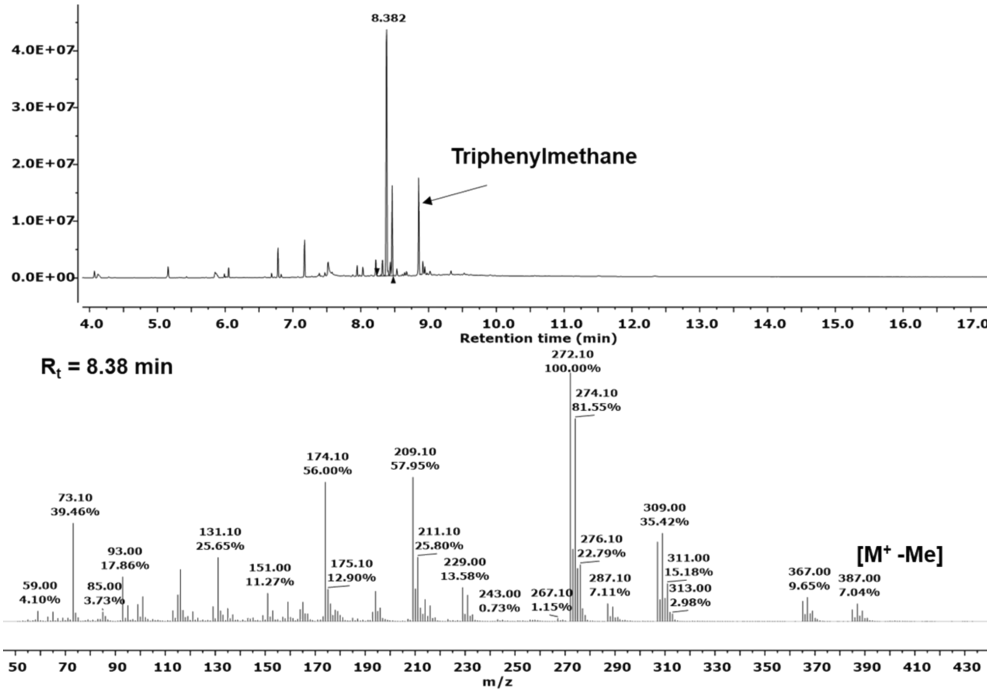

**Figure S 21.** GCMS of the reaction mixture and MS spectrum of the main component **7**.

**Reaction conditions: DCM, –90 °C, 2.0 equiv. [Ph$_3$C][B(C$_6$F$_5$)$_4$]**

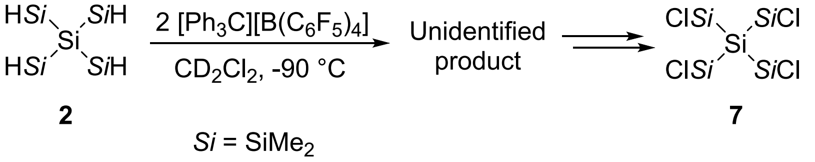

The same reaction was attempted with a ratio **2** : [Ph$_3$C][B(C$_6$F$_5$)$_4$] = 1 : 2. A solution of the pentasilane **2** (1.00 equiv., 0.06 mmol) in dichloromethane-d$_2$ (0.3 mL) was added to an NMR tube containing the solution of [Ph$_3$C][B(C$_6$F$_5$)$_4$] (2.00 equiv., 0.12 mmol) in dichloromethane-d$_2$ (0.3 mL) at –90 °C. The spectroscopic data did not show significant differences compared to the reaction using a 1 : 1 ratio except for more left-over trityl cation. The mixture was also removed from the NMR spectrometer, newly mixed, and returned to the spectrometer. The formation of the chlorosilane **7** as well as the decomposition of Ph$_3$CH were observed.

For the spectroscopic data of chlorosilane **7**, see reaction with 1 : 1 stoichiometry.

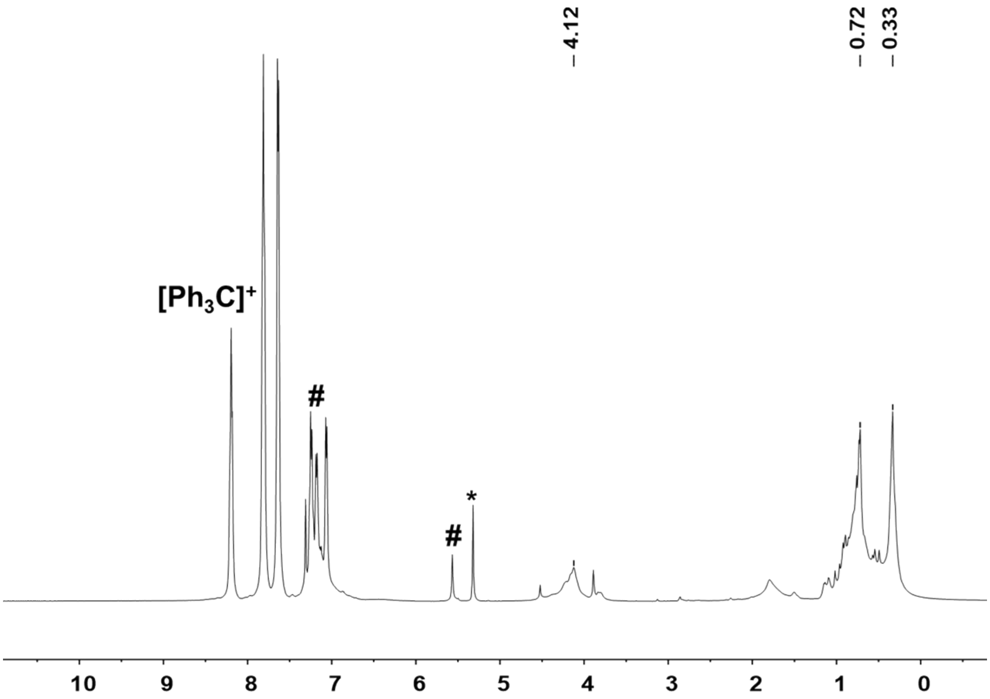

**Figure S 22.** $^1$H NMR spectrum prior to renewed mixing ($CD_2Cl_2$, 499.87 MHz, 183.1 K, * = $CDHCl_2$, # = $Ph_3CH$).

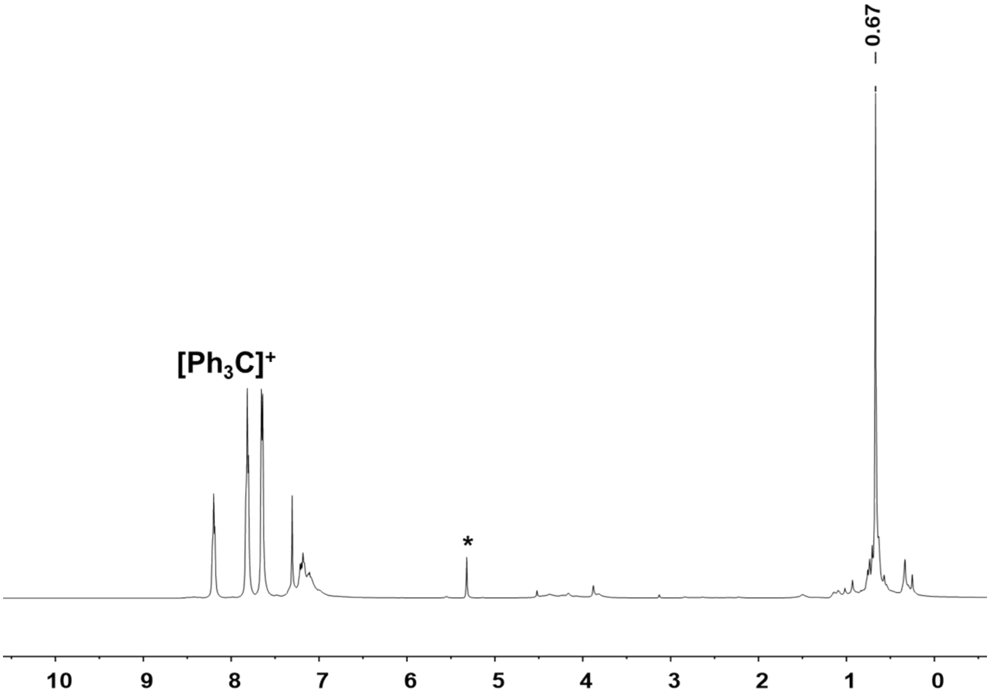

**Figure S 23.** $^1$H NMR spectrum after renewed mixing ($CD_2Cl_2$, 499.87 MHz, 183.1 K, * = $CDHCl_2$).

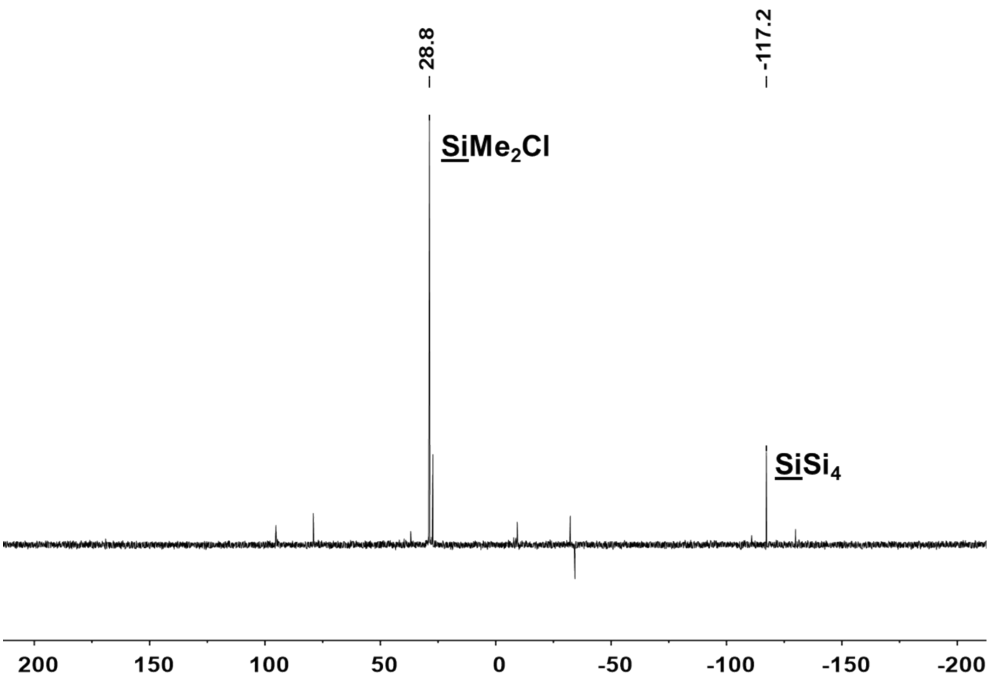

**Figure S 24.** $^{29}$Si{$^1$H} INEPT NMR spectrum renewed mixing ($CD_2Cl_2$, 99.31 MHz, 183.1 K).

## Reaction conditions: 3-F-tol, –80 °C, 0.5 equiv. [$Ph_3C$][$B(C_6F_5)_4$]

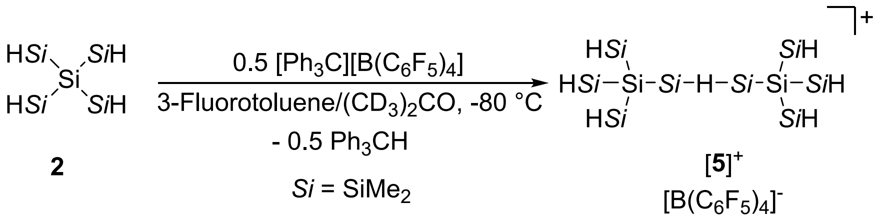

The general procedure was applied for the hydride transfer reaction between **2** and [$Ph_3C$][$B(C_6F_5)_4$] in a 1 : 0.5 stoichiometry using 3-F-tol as solvent. The trityl salt, [$Ph_3C$][$B(C_6F_5)_4$] (1.00 equiv., 0.07 mmol), was dissolved in 3-F-tol (0.3 mL) in an NMR tube and cooled down. Subsequently, a solution of silane **2** (1.00 equiv., 0.14 mmol) in 3-F-tol (0.3 mL) was slowly added at –80 °C via syringe. The NMR tube was additionally equipped with a capillary filled with the NMR solvent acetone-$d_6$. The recorded NMR spectra showed the formation of the intermolecularly bridged silyl cation [**5**]$^+$ which was also obtained after the reaction of equimolar amounts silane and trityl salt.

Analytical data of [**5**][$B(C_6F_5)_4$]

$^1$H NMR (3-F-tol/$(CD_3)_2CO$, 499.87 MHz, 193.0 K): 0.32 (bs, Si$\underline{Me_2}$H), 0.76 (bs, $\underline{Me_2}$Si-H-Si$\underline{Me_2}$), 4.23 (bs, SiMe$_2\underline{H}$). $^{13}$C{$^1$H} NMR (3-F-tol/$(CD_3)_2CO$, 125.71 MHz, 193.0 K): –2.9 (s, Si$\underline{Me_2}$H), 1.4 (s, $\underline{Me_2}$Si-H-Si$\underline{Me_2}$). $^{29}$Si{$^1$H} NMR (3-F-tol/$(CD_3)_2CO$, 99.31 MHz, 193.0 K): –133.3 (bs, $\underline{Si}Si_4$), –34.0 (bs, $\underline{Si}$Me$_2$H), 93.1 (bs, Me$_2\underline{Si}$-H-$\underline{Si}$Me$_2$).

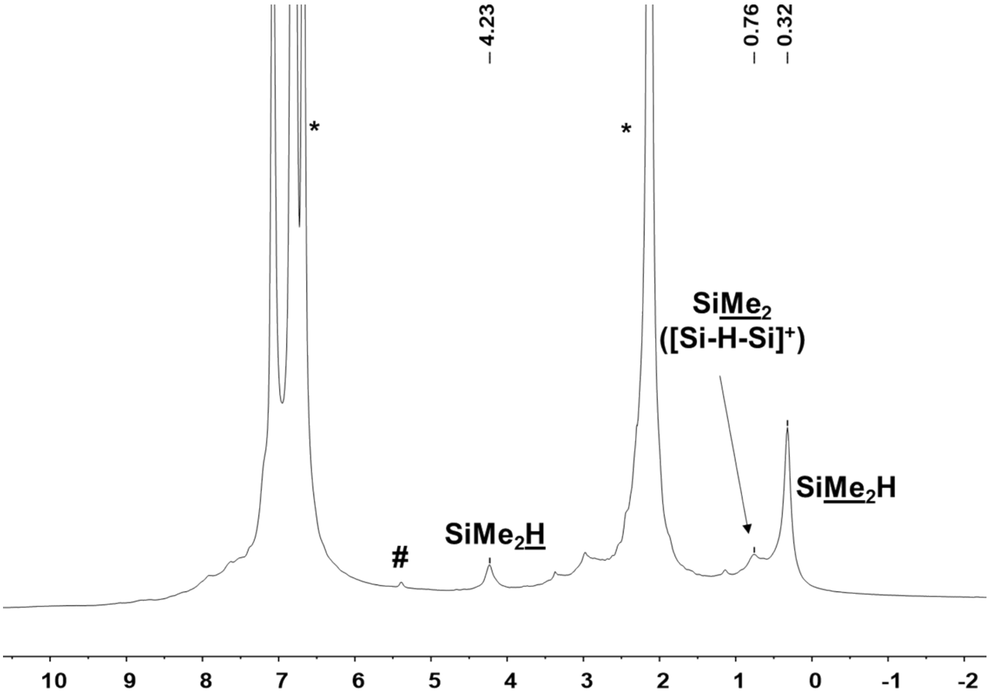

**Figure S 25.** $^1$H NMR spectrum of [**5**][B($C_6F_5$)$_4$] (3-F-tol, 499.87 MHz, 193.0 K, * = 3-F-tol, # = $Ph_3CH$).

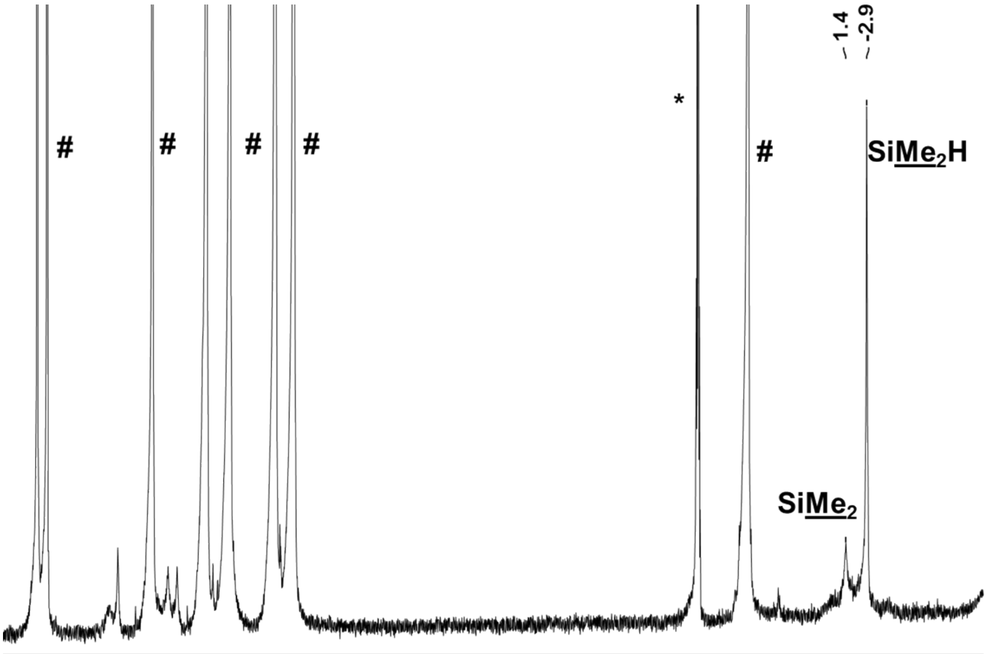

**Figure S 26.** $^{13}$C{$^1$H} NMR spectrum of [**5**][B($C_6F_5$)$_4$] (3-F-tol, 125.71 MHz, 193.0 K, # = 3-F-tol, * = $Ph_3CH$).

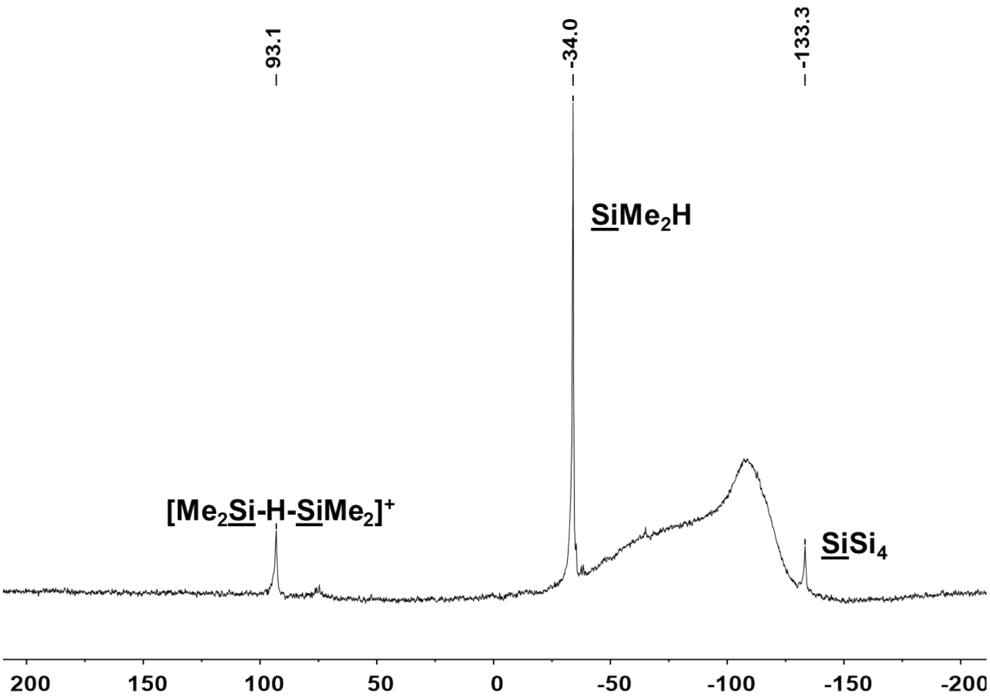

**Figure S 27.** $^{29}$Si{$^{1}$H} NMR spectrum of [**5**][$B(C_6F_5)_4$] (3-F-tol/$(CD_3)_2CO$, 99.31 MHz, 193.0 K).

### Reaction conditions: 3-F-tol, –80 °C, 1.0 equiv. [$Ph_3C$][$B(C_6F_5)_4$]

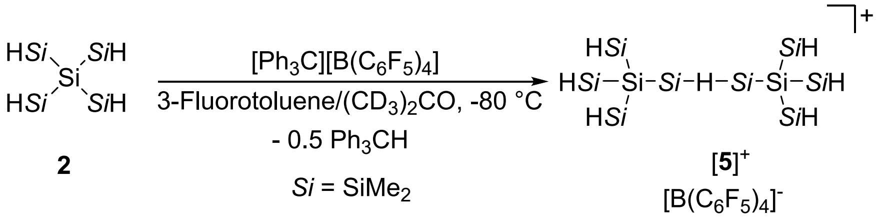

The general procedure was applied for the hydride transfer reaction between equimolar amounts of pentasilane **2** and [$Ph_3C$][$B(C_6F_5)_4$] in 3-F-tol. The trityl salt, [$Ph_3C$][$B(C_6F_5)_4$] (1.00 equiv., 0.08 mmol), was dissolved in 3-F-tol (0.3 mL) in an NMR tube and cooled down. Subsequently, a solution of silane **2** (1.00 equiv., 0.08 mmol) in 3-F-tol (0.3 mL) was slowly added at –80 °C via syringe. The NMR tube was additionally equipped with a capillary filled with acetone-$d_6$. The obtained NMR spectra showed the clean formation of one product. Analysis of the spectroscopic data revealed the formation of the intermolecularly stabilised silyl cation [**5**]$^+$.

Analytical data of [**5**][$B(C_6F_5)_4$]

$^{1}$H NMR (3-F-tol/$(CD_3)_2CO$, 499.87 MHz, 192.9 K): 0.32 (s, 36H, Si$Me_2$H), 0.79 (s, 12H, $Me_2$Si-H-Si$Me_2$), 4.22 (s, 6H, Si$Me_2$H). $^{13}$C{$^{1}$H} NMR (3-F-tol/$(CD_3)_2CO$, 125.71 MHz, 193.0 K): –2.9 (s, Si$Me_2$H), 1.4 (s, $Me_2$Si-H-Si$Me_2$), $^{13}$C signals of [$B(C_6F_5)_4$]$^-$ not assigned. $^{11}$B{$^{1}$H} NMR (3-F-tol/$(CD_3)_2CO$, 160.38 MHz, 193.1 K): –17.5 (s, [$B(C_6F_5)_4$]$^-$). $^{19}$F{$^{1}$H} NMR (3-F-tol/$(CD_3)_2CO$, 470.28 MHz, 193.1 K): –167.02 (bs, [$B(C_6F_5)_4$]$^-$), –162.92 (bs, [$B(C_6F_5)_4$]$^-$), –133.28 (bs, [$B(C_6F_5)_4$]$^-$). $^{29}$Si{$^{1}$H} NMR (3-F-tol/$(CD_3)_2CO$, 99.31 MHz, 193.0 K): –133.2 (s, $SiSi_4$), –34.0 (s, $SiMe_2H$), 93.1 (s, $Me_2$Si-H-Si$Me_2$). $^{29}$Si NMR (3-F-tol/$(CD_3)_2CO$, 99.31 MHz, 193.0 K): –133.2 (s, $SiSi_4$), –34.0 (d, $^{1}J_{Si,H}$ = 185 Hz, $SiMe_2H$), 93.1 (d, $^{1}J_{Si,H}$ = 49 Hz, $Me_2$Si-H-Si$Me_2$).

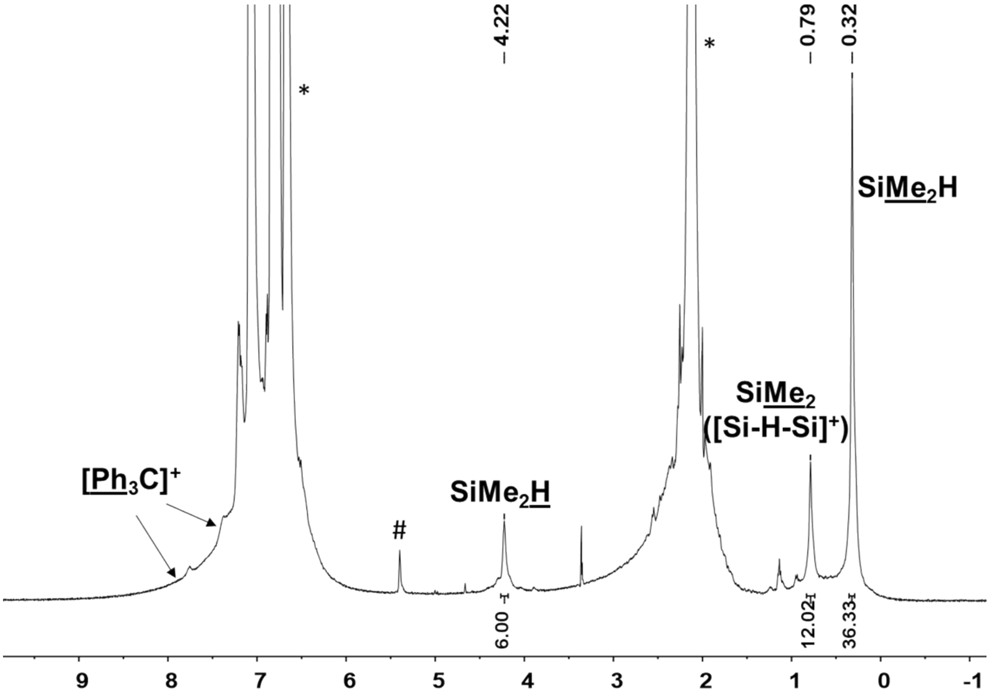

**Figure S 28.** $^1$H NMR spectrum of [**5**][B($C_6F_5$)$_4$] (3-F-tol, 499.87 MHz, 192.9 K, * = 3-F-tol, # = $Ph_3CH$).

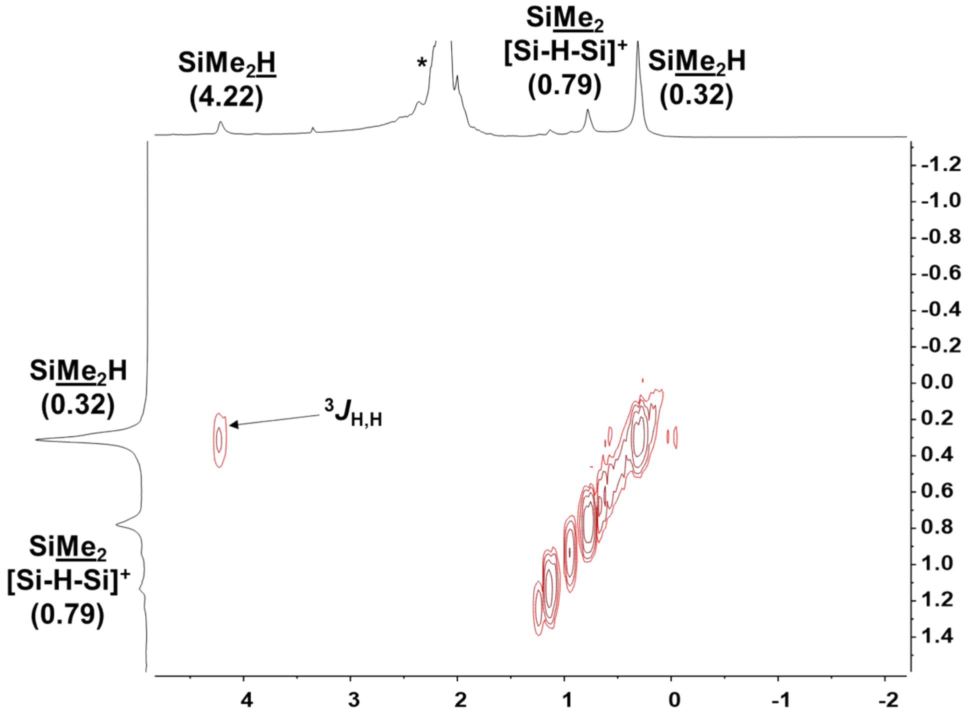

**Figure S 29.** Excerpt of the $^1$H,$^1$H COSY NMR spectrum of [**5**][B($C_6F_5$)$_4$] (3-F-tol, 499.87 MHz, 192.9 K).

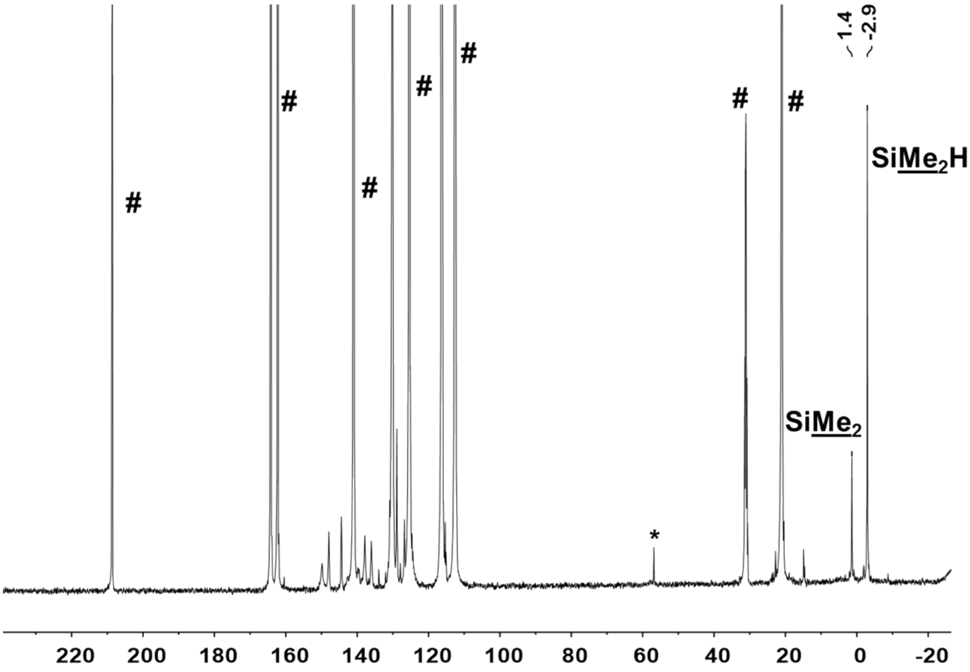

**Figure S 30.** $^{13}C\{^{1}H\}$ NMR spectrum of [**5**][$B(C_6F_5)_4$] (3-F-tol, 125.71 MHz, 193.0 K, # = 3-F-tol and $(CD_3)_2CO$, * = $Ph_3CH$).

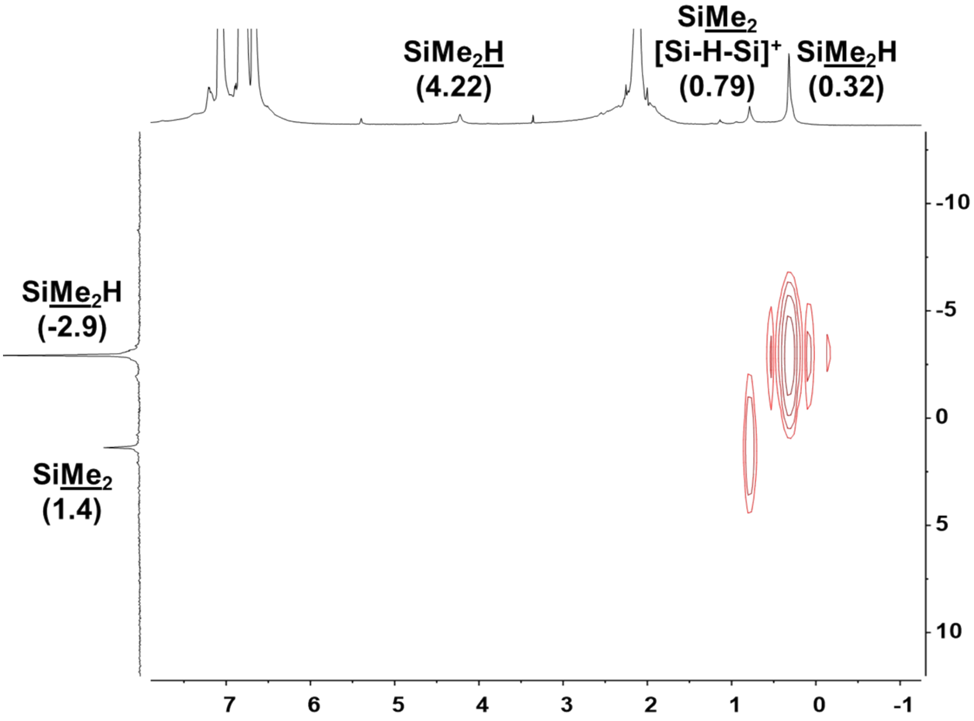

**Figure S 31.** Excerpt of the $^{1}H,^{13}C$ HMQC NMR spectrum of [**5**][$B(C_6F_5)_4$] (3-F-tol, 499.87 MHz, 192.9 K).

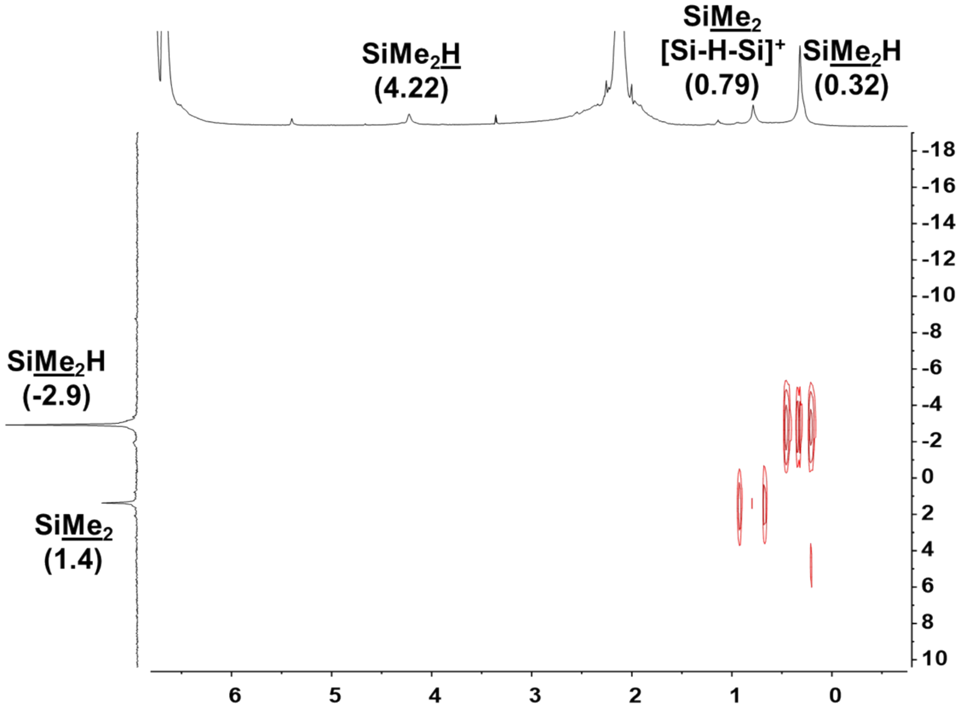

**Figure S 32.** Excerpt of the $^1$H,$^{13}$C HMBC NMR spectrum of [**5**][B(C$_6$F$_5$)$_4$] (3-F-tol, 499.87 MHz, 192.9 K).

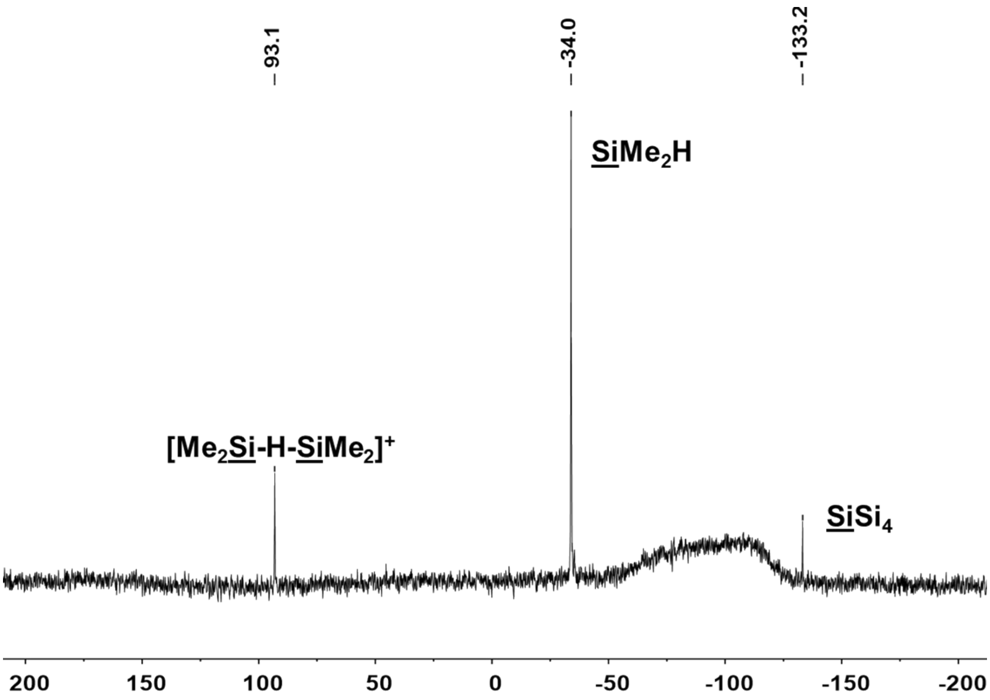

**Figure S 33.** $^{29}$Si{$^1$H} NMR spectrum of [**5**][B(C$_6$F$_5$)$_4$] (3-F-tol, 99.31 MHz, 193.0 K).

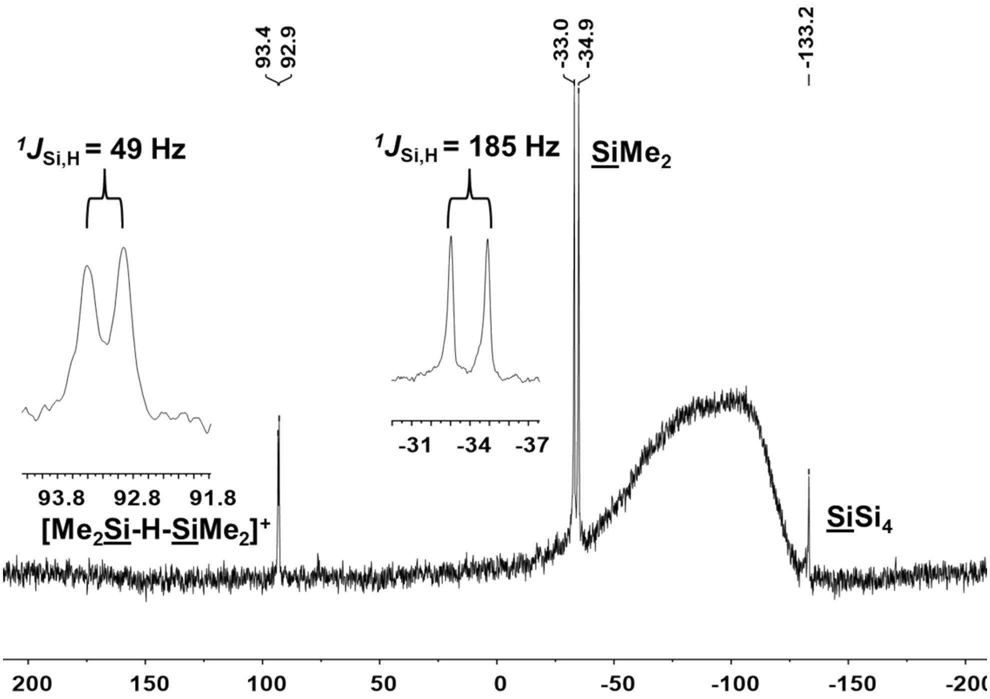

**Figure S 34.** $^{29}$Si NMR spectrum of [**5**][B(C$_6$F$_5$)$_4$] (3-F-tol, 99.31 MHz, 193.0 K).

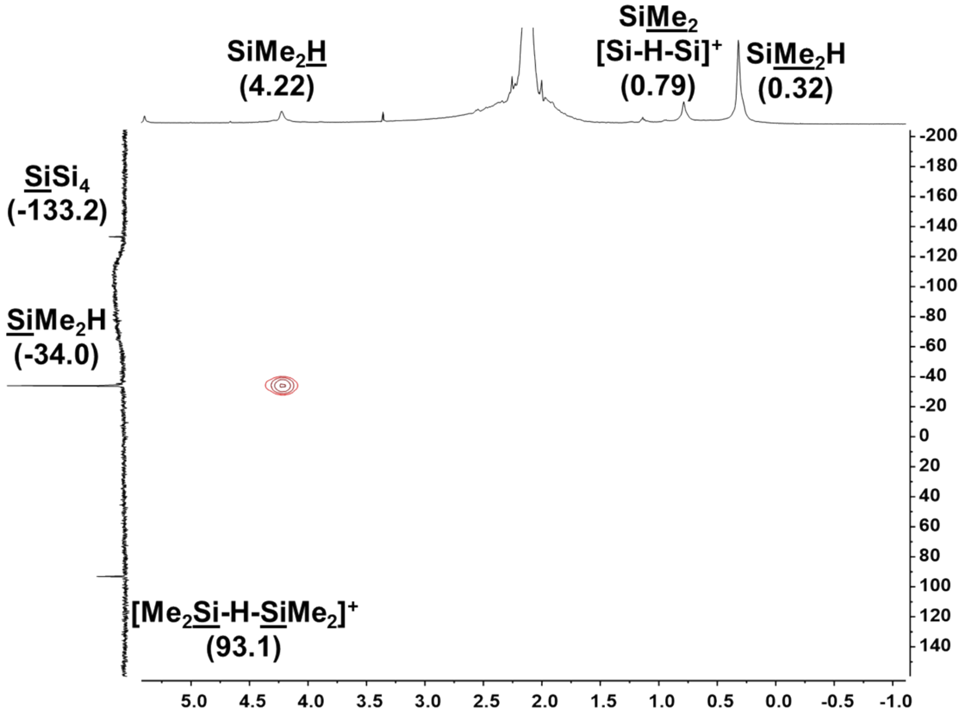

**Figure S 35.** Excerpt of the $^1$H,$^{29}$Si HMQC NMR spectrum of [**5**][B(C$_6$F$_5$)$_4$] (3-F-tol, 499.87 MHz, 193.0 K).

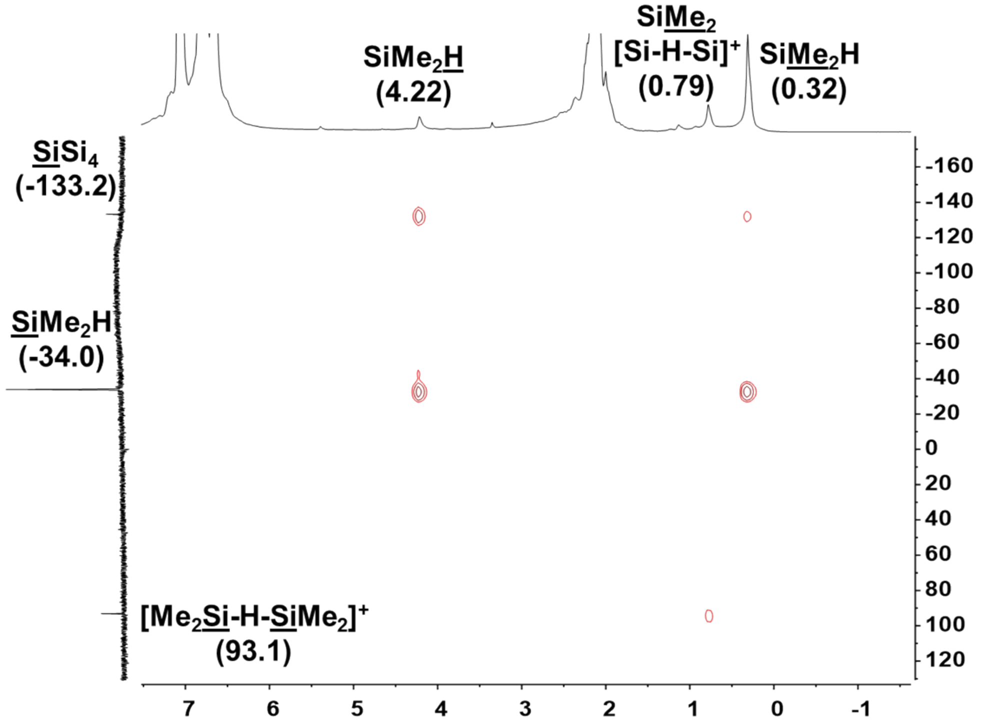

**Figure S 36.** Excerpt of the $^1$H,$^{29}$Si HMQC NMR spectrum of [**5**][B(C$_6$F$_5$)$_4$] (3-F-tol, 499.87 MHz, 193.0 K, optimised for *J* = 50 Hz).

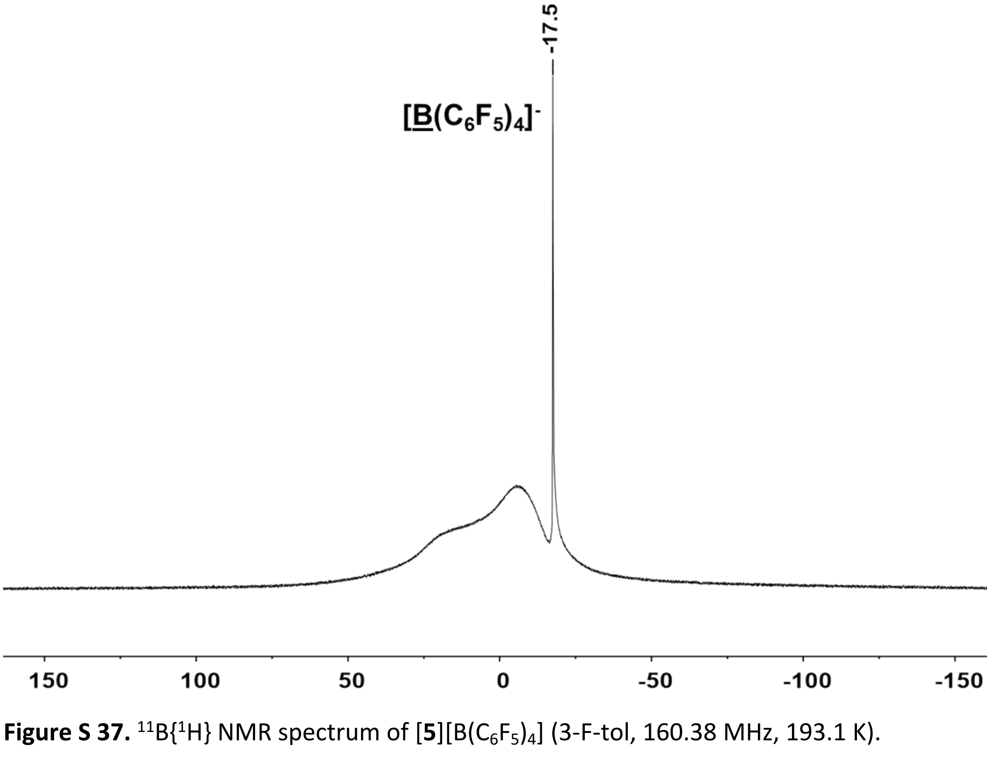

**Figure S 37.** $^{11}$B{$^1$H} NMR spectrum of [**5**][B(C$_6$F$_5$)$_4$] (3-F-tol, 160.38 MHz, 193.1 K).

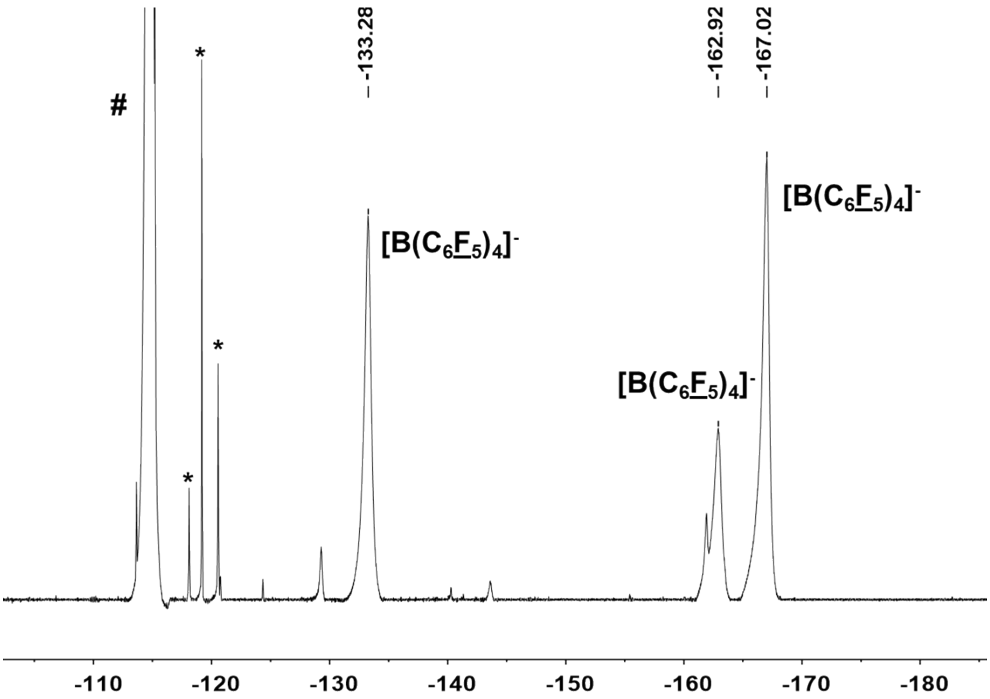

**Figure S 38.** $^{19}F\{^1H\}$ NMR spectrum of [**5**]$[B(C_6F_5)_4]$ (3-F-tol, 470.28 MHz, 193.1 K, # = 3-F-tol, * = impurities in 3-F-tol).

## Reaction conditions: 3-F-tol, –80 °C, 2.0 equiv. $[Ph_3C][B(C_6F_5)_4]$

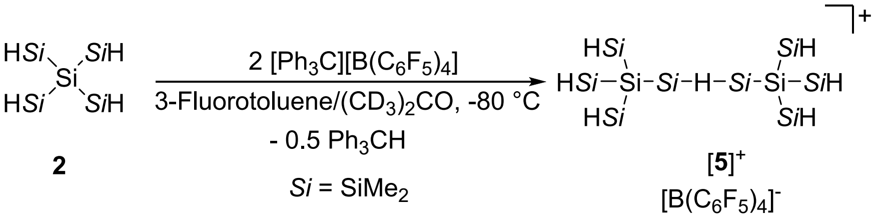

The reaction was performed analogously to the procedure described for the 1 : 1 stoichiometry of pentasilane **2** and trityl salt. The trityl salt, $[Ph_3C][B(C_6F_5)_4]$ (2.00 equiv., 0.08 mmol), was dissolved in 3-F-tol (0.3 mL) in an NMR tube and cooled down. Subsequently, a solution of silane **2** (1.00 equiv., 0.04 mmol) in 3-F-tol (0.3 mL) was slowly added at –80 °C via syringe. The NMR tube was additionally equipped with a capillary filled with the NMR solvent acetone-$d_6$. The NMR spectra indicated the formation of the intermolecularly bridged silyl cation [**5**]$^+$.

Analytical data of [**5**] $[B(C_6F_5)_4]$

$^1H$ NMR (3-F-tol/$(CD_3)_2CO$, 499.87 MHz, 193.0 K): 0.32 (s, $Si\underline{Me_2}H$), 0.79 (s, $\underline{Me_2}Si$-H-$Si\underline{Me_2}$), 4.23 (s, $SiMe_2\underline{H}$). $^{29}Si\{^1H\}$ NMR (3-F-tol/$(CD_3)_2CO$, 99.31 MHz, 193.0 K): –133.3 (s, $\underline{Si}Si_4$), –33.9 (s, $\underline{Si}Me_2H$) 93.1 (s, $Me_2\underline{Si}$-H-$\underline{Si}Me_2$).

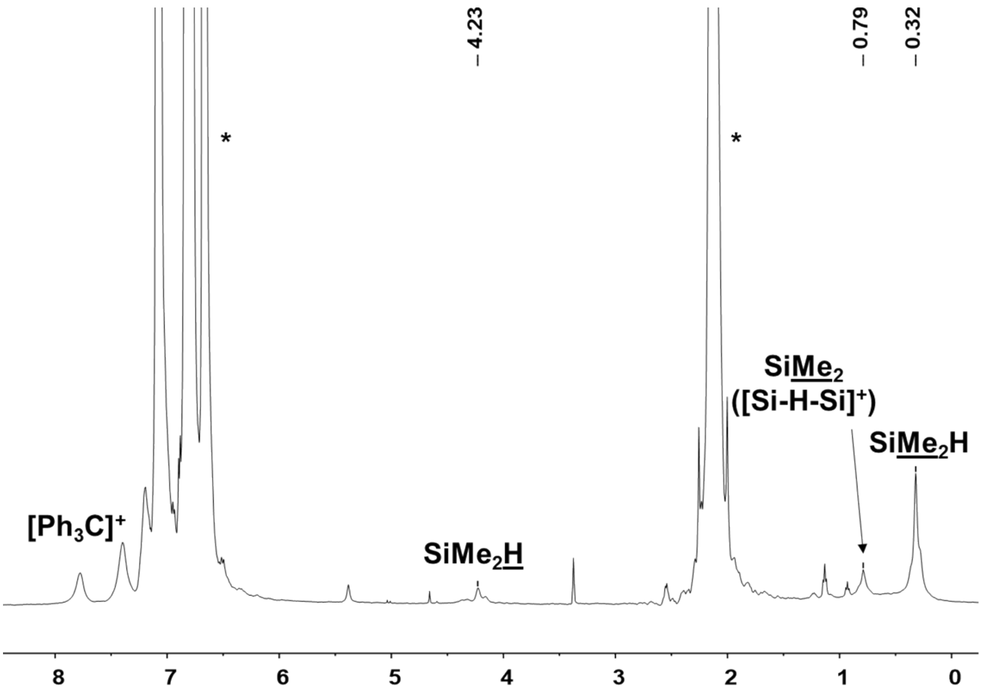

**Figure S 39.** $^1$H NMR spectrum of [**5**][B($C_6F_5$)$_4$] (3-F-tol/($CD_3$)$_2$CO, 499.87 MHz, 193.0 K, * = 3-F-Tol).

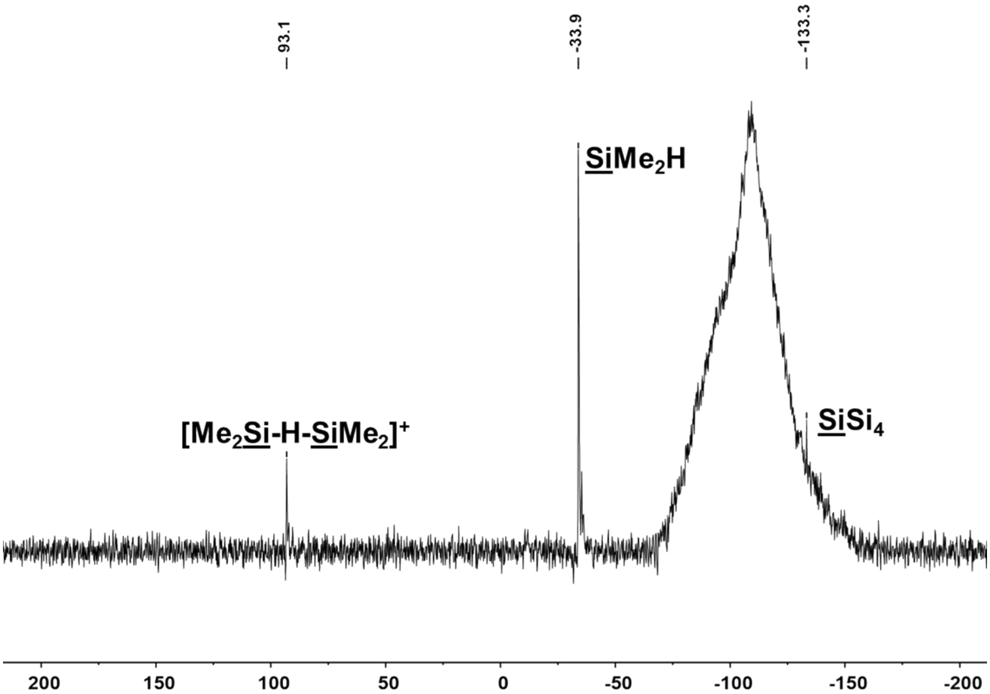

**Figure S 40.** $^{29}$Si{$^1$H} NMR spectrum of [**5**][B($C_6F_5$)$_4$] (3-F-tol, 99.31 MHz, 193.0 K).

# Computational Results

**Pressure correction of Gibbs free energies values for reactions in 3-F-Tol**

In general, the values for the Gibbs free energy ΔG were first computed at physical parameters of 298 K and 101325 Pa ($G^{298}$). A correction of the data computed at 298 K and 101325 Pa, that was proposed by Martin and co-workers,[7] was subsequently applied using Gaussian's *freqchk* utility. According to the equation $p = \rho RT$ and the respective density of the used solvent the respective pressure and temperature corrections were applied.

For 3-F-tol a density of ρ = 9991 kg m$^{-3}$ was assumed. Hence, for a temperature of 193 K, a pressure of 14.49 MPa was computed. Corrected values are marked with an additional asterisk (ΔG*).

### Computations of NMR chemical shifts and $^{1}J_{Si,H}$ coupling constants

For referencing of the NMR chemical shifts, the magnetic shielding tensors of tetramethylsilane (TMS) were computed at the GIAO/M06-L/6-311G(2d,p)//M06-2X/6-311+G(d,p) level of theory. The computed parameters of [**4**]$^+$ and [**5**]$^+$ are given relative to these values. The $^{1}J_{Si,H}$ coupling constants were computed from the optimised structures at the B3LYP/IGLOIII//M06-2X/6-311+G(d,p) level of theory.

### Details on the computed structures

All structures were computed using Gaussian 16 Revision A.03.[8] If not specifically mentioned, the structures were all computed at the M06-2X/6-311+G(d,p) level of theory. Stationary points were verified by frequency calculations.

The computed energies of the model compounds that were used to compare intramolecular vs. intermolecular Si-H-Si bridge formation are summarised in Table S 3, while Table S 4 shows the influence of temperature on the Gibbs free energy values of the isodesmic reaction used to evaluate the stability of different cyclic Si-H-Si bridged cations.

**Table S 3.** Computed energies for the estimation of ring strain energies and the formation of 3c2e Si-H-Si bridges.

| Compound | n (SiMe$_2$) | E [a.u] | G$^{298}$ [a.u] | NImag |
|---|---|---|---|---|
| SiMe$_3$H | - | –409.80754 | –409.71815 | 0 |
| 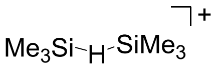 [**VII**]$^+$ | - | –818.78717 | –818.59757 | 0 |
| 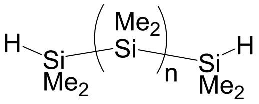 | 0 | –739.79868 | –739.67038 | 0 |
| | 1 | –1109.11283 | –1108.91837 | 0 |
| | 2 | –1478.42804 | –1478.16525 | 0 |
| | 3 | –1847.74333 | –1847.41339 | 0 |
| | 4 | –2217.05884 | –2216.66067 | 0 |
| | 5 | –2586.37422 | –2585.90884 | 0 |
| 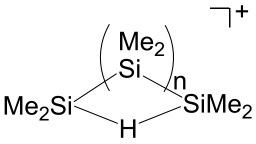 [**I**]$^+$-[**VI**]$^+$ | 0 | –738.920117 | –738.800144 | 0 |
| | 1 | –1108.26555 | –1108.07598 | 0 |
| | 2 | –1477.59641 | –1477.33902 | 0 |
| | 3 | –1846.92007 | –1846.59490 | 0 |
| | 4 | –2216.24052 | –2215.84525 | 0 |
| | 5 | –2585.56065 | –2585.09449 | 0 |
| [**VIII**]$^+$ | 1 | -1344.08430 | -1343.72820 | 0 |
| [**VIII**]-H | 1 | -1344.93190 | -1344.56823 | 0 |

**Table S 4.** Summary of the energies computed for the isodesmic reaction to evaluate the stability of cyclic Si-H-Si bridged silyl cations at variable temperatures.

| Cation | n | Ring size | ΔE [kJ mol$^{-1}$] | ΔG$^{373}$ [kJ mol$^{-1}$] | ΔG$^{298}$ [kJ mol$^{-1}$] | ΔG$^{183}$ [kJ mol$^{-1}$] | ΔG$^{153}$ [kJ mol$^{-1}$] | ΔG$^{93}$ [kJ mol$^{-1}$] |
|---|---|---|---|---|---|---|---|---|
| **[I]**$^+$ | 0 | 3 | 133 | 74 | 83 | 101 | 105 | 115 |
| **[II]**$^+$ | 1 | 4 | 51 | 0 | 10 | 25 | 29 | 37 |
| **[III]**$^+$ | 2 | 5 | 10 | –42 | –32 | –18 | –13 | –5 |
| **[IV]**$^+$ | 3 | 6 | –12 | –62 | –53 | –39 | –35 | –27 |
| **[V]**$^+$ | 4 | 7 | –25 | –69 | –61 | –48 | –45 | –38 |

| | | | | | | | | |
|---|---|---|---|---|---|---|---|---|
| **[VI]**$^+$ | 5 | 8 | −38 | −69 | −63 | −55 | −52 | −47 |

Figure S 41 shows a plot of the Gibbs free energy of isodesmic reaction for the formation of the intramolecularly bridged cation **[III]**$^+$ depending on the temperature. The computations predict the reaction to become thermoneutral around −215 °C (58 K) and endergonic at even lower temperatures.

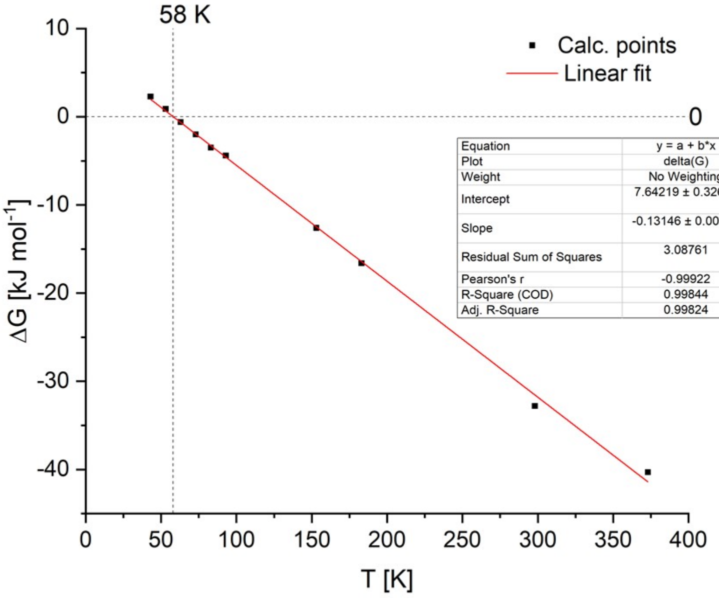

**Figure S 41.** Plot of ΔG vs. T for the Gibbs free energy of the isodesmic reaction resulting in the formation of cation [**III**]$^+$..

We also estimated the contribution of the Thorpe-Ingold effect by the computation of the isodesmic reaction for the formation of [**VIII**]$^+$, an analogous compound to [**II**]$^+$ but with a central $Si^tBu_2$ group instead of $SiMe_2$ (Scheme S 1). With the bulkier *tert*-butyl substituents at the central silicon atom, our calculation still reveal the reaction to be endothermic (ΔE = 52 kJ mol$^{-1}$) as well as endergonic ($\Delta G^{298}$ = 3 kJ mol$^{-1}$).

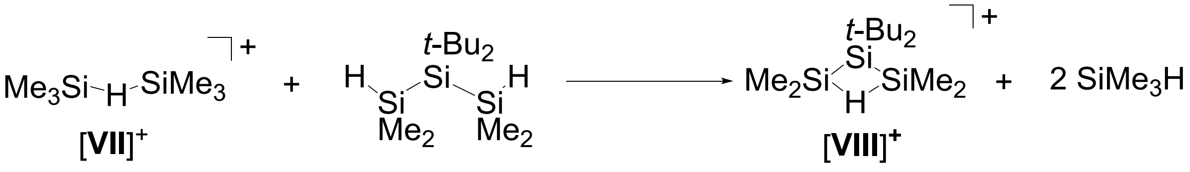

**Scheme S 1.** Isodesmic reaction used to evaluate the influence of bulkier substituents.

The energies of the neutral starting compound **2**, the non-bridged silylium ion [**3**]$^+$, the intramolecularly bridged cation [**4**]$^+$ as well as the intermolecularly bridged cation [**5**]$^+$ are summarised in Table S 5.

**Table S 5.** Computed energies of starting material **2**, Si-H-Si bridged cation [**4**]$^+$ and [**5**]$^+$ and non-bridged silylium ion [**3**]$^+$.

| Compound | E [a.u] | $G^{298}$ [a.u] | $G^{*198}$ [a.u] | NImag |
|---|---|---|---|---|
| **2** | −1769.12102 | −1767.84137 | −1767.96204 | 0 |
| [**3**]$^+$ | −1768.26299 | −1767.99168 | −1767.96206 | 0 |
| [**4**]$^+$ | −1768.27918 | −1768.00724 | −1767.97753 | 0 |
| [**5**]$^+$ | −3537.43662 | −3536.85741 | −3536.81019 | 0 |

The corresponding structures are pictured in Figure S 42 and important structural parameters of the 3c2e Si-H-Si bridges of the bridged cations [**4**]$^+$ and [**5**]$^+$ are summarised in Table S 6. The optimized molecular structures are given in the file cations_3-5.xyz, readable with the mercury/CCDC visualization software.

**Table S 6.** Comparison of computed structural parameters of the 3c2e Si-H-Si bridge in cations [**4**]$^+$ and [**5**]$^+$.

| Compound | d(Si-H) [pm] | d(Si-Si) [pm] | α(Si-H-Si) [°] | Σα [°] |
|---|---|---|---|---|
| [**4**]$^+$ | 168 | 266 | 105 | 356 |
| [**5**]$^+$ | 162/163 | 318 | 157 | 347 |

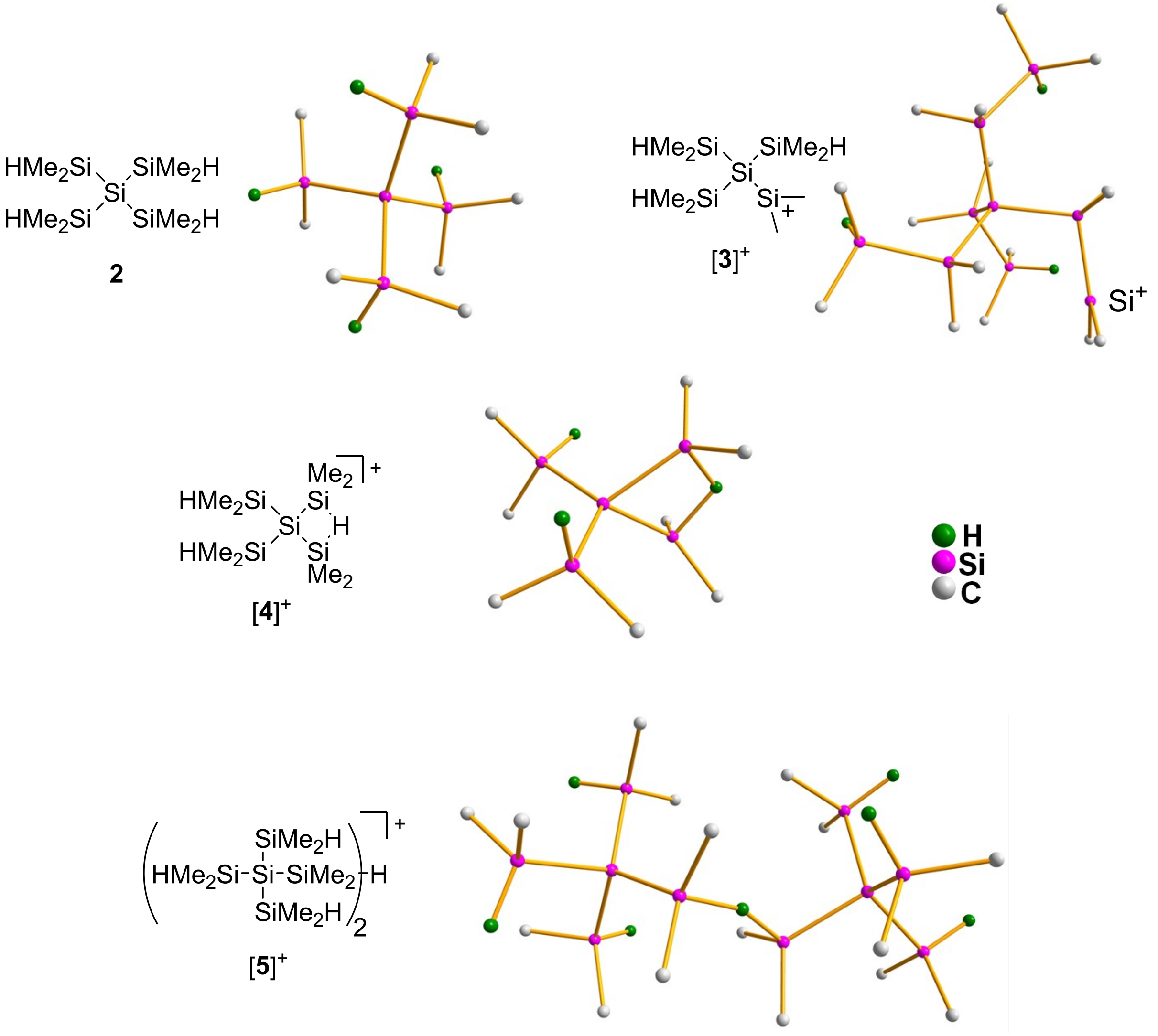

**Figure S 42.** Optimzed molecular structures of the neutral starting material **2**, the non-bridged silylium ion [**3**]$^+$and the bridged cation [**4**]$^+$-[**5**]$^+$, (M06-2X/6-311+G(d,p), methyl hydrogen atoms are not shown).

# Literature

1 G. R. Fulmer, A. J. M. Miller, N. H. Sherden, H. E. Gottlieb, A. Nudelman, B. M. Stoltz, J. E. Bercaw and K. I. Goldberg, *Organometallics*, 2010, **29**, 2176-2179.

2 H. Gilman and C. L. Smith, *J. Organomet. Chem.*, 1967, **8**, 245-253.

3 K. Trommer, U. Herzog and G. Roewer, *J. Prakt. Chem.*, 1997, **339**, 637-641.

4 P. Kulpiński, P. D. Lickiss and W. Stańczyk, *Bull. Pol. Acad. Sci. Chem.*, 1992, **40**, 21.

5 U. Herzog and G. Roewer, *J. Organomet. Chem.*, 1997, **527**, 117-124.

6 E. Ihara, V. G. Young and R. F. Jordan, *J. Am. Chem. Soc.*, 1998, **120**, 8277-8278.

7 R. L. Martin, P. J. Hay and L. R. Pratt, *J. Phys. Chem. A*, 1998, **102**, 3565-3573.

8 Gaussian 16, Revision A.03, M. J. Frisch, G. W. Trucks, H. B. Schlegel, G. E. Scuseria, M. A. Robb, J. R. Cheeseman, G. Scalmani, V. Barone, G. A. Petersson, H. Nakatsuji, X. Li, M. Caricato, A. V. Marenich, J. Bloino, B. G. Janesko, R. Gomperts, B. Mennucci, H. P. Hratchian, J. V. Ortiz, A. F. Izmaylov, J. L. Sonnenberg, D. Williams-Young, F. Ding, F. Lipparini, F. Egidi, J. Goings, B. Peng, A. Petrone, A. Petrone, T. Henderson, D. Ranasinghe, V. G. Zakrzewski, J. Gao, N. Rega, G. Zheng, W. Liang, M. Hada, M. Ehara, K. Toyota, R. Fukuda, J. Hasegawa, M. Ishida, T. Nakajima, Y. Honda, O. Kitao, H. Nakai, T. Vreven, K. Throssell, J. A. Montgomery, Jr., J. E. Peralta, F. Ogliaro, M. J. Bearpark, J. J. Heyd, E. N. Brothers, K. N. Kudin, V. N. Staroverov, T. A. Keith, R. Kobayashi, J. Normand, K. Raghavachari, A. P. Rendell, J. C. Burant, S. S. Iyengar, J. Tomasi, M. Cossi, J. M. Millam, M. Klene, C. Adamo, R. Cammi, J. W. Ochterski, R. L. Martin, K. Morokuma, O. Farkas, J. B. Foresman and D. J. Fox, Gaussian, Inc., Wallingford CT, 2016.